

Barking Up the Right Tree: Evidence for reduction in xylem embolism due to bark water uptake in Bigleaf Maple, Douglas-fir, and Coast Redwood

A Thesis

Presented to

The Division of Mathematics and Natural Sciences

Reed College

In Partial Fulfillment

of the Requirements for the Degree

Bachelor of Arts

Annapurna Post-Leon

May 2020

Approved for the Division

(Biology)

Aaron Ramirez

Acknowledgments

First and foremost, I would like to thank my parents and my sister Sequoia for their unconditional love, support, and humor through all the ups and downs of the last four years. Thank you also to my wonderful Aunt Cindy, and my loving Baboo. I love you!

A special thanks to all the members of the Ramirez Lab. Thank you especially to my advisor, Aaron Ramirez, for your support and guidance throughout my thesis and summer research. I couldn't have asked for a better mentor. Thank you to Hannah Prather, for your encouragement, support, and attempts to fix the centrifuge. And, of course, thank you to all the other thesising seniors of the lab: Claire, Maia, Caleb, and Ariel, who will be graduating with me, and Piper, Edward, Erica, and Indra, who graduated last year. Thank you all for being a wonderful, supportive group of people to be in the lab and field with!

Thank you to the Reed Biology department, and all of the professors, staff, and students who make it great. Thank you to Kristy Gonyer, whose organizational skills, kindness, and endless supply of chocolate helped me make it through. Thanks to all the members of the B101 thesis office: Gabe, Jamie, Maddox, Karl, Carter, Jesse, Sol, Olivia, and Aidan. We did it!

Last, but definitely not least, thank you to my friends. Thanks to Lorelee Bandy, whose support and commiseration got me through four years at Reed, and to Nicole Kretekos, Katherine Draves, Paul Molamphy, Russ Foust, and the other *Quest*, *Quest*-adjacent, and *Quest*-unaffiliated people who have been wonderful editors and friends. Thank you to my outstanding housemates in Brag Haus, past and present: Thomas Malthouse, Shawn Owens, Claire Jellison, and Sophia Kongshaug. I can't believe it's been four years already.

Preface

The Pacific Northwest follows an unusual climate pattern of very wet, mild winters and hot, dry summers, which has led to an abundance of dense forests dominated by evergreen conifers at latitudes much lower than in other parts of the world. These forests are home to two of the tallest tree species in the world, Coast Redwood and Douglas-fir, both which have been recorded at heights well over 100 meters. Other species native to the Pacific Northwest, like Bigleaf Maple, are not quite as tall but are still the largest specimens of their genus; Bigleaf Maple is particularly notable due to its ability to host canopy moss and lichen mats rivalling those of the tropics. However, climate change threatens these tall forests with a hotter, drier future. The survival of the forests of the Pacific Northwest will depend on the ability of tree species to adapt to longer periods of hotter drought. This thesis explores bark water absorption as a potential avenue of hydraulic recovery for trees that will receive less rainfall but still experience summer fog, or have water-holding epiphyte masses that keep bark damp in dry conditions.

List of Abbreviations

ANOVA	Analysis of variance
J	Joule (unit of energy)
K_h	Stem-specific xylem hydraulic conductance
K_{h,max}	K _h after vacuum infiltration
K_{h,min}	K _h after centrifugation or drydown
K_{h,post-treatment}	K _h after treatment
K_s	Stem-specific xylem hydraulic conductivity
K_{s,max}	K _s after vacuum infiltration
K_{s,min}	K _s after centrifugation or drydown
K_{s,post-treatment}	K _s after treatment
mg mm⁻¹ s⁻¹ kPa	Unit of stem-specific hydraulic conductivity
MPa	Megapascal (unit of pressure)
PLC	Percent loss in conductivity
PLC_{min}	PLC after centrifugation or drydown
PLC_{post-treatment}	PLC after treatment
Ψ_w	Water potential

For additional information on the definitions of abbreviations and other terms used in this thesis, please see Appendix A.

Table of Contents

Chapter 1: The Climate and Forests of the Pacific Northwest.....	1
Mediterranean Climates and the Conifer-Dominated Forests of the Pacific Northwest	1
Coast Redwood, Douglas-fir, Bigleaf Maple, and Epiphytes.....	5
Climate Change and the Role of Hotter Drought	11
Chapter 2: Plant Hydraulics and the Tall-Tree Problem	15
The Biophysics of Water in Plants	15
Water Movement in Plants and the Cohesion-Tension Theory	18
Xylem Embolism, Measurement of Cavitation, and Embolism Repair	21
Canopy Water Uptake and the Tall-Tree Problem	24
Chapter 3: Methods	27
Site Selection	27
Epiphyte Massing and Branch Age Methods	27
Dye Infiltration Methods	28
Measurement of Hydraulic Conductivity	28
Centrifugation Methods	29
Benchtop Drydown Methods	31
Calculations	33
Statistical Analyses	33
Chapter 4: Results.....	35
Branch Age and Epiphyte Massing Results.....	35
Dye Infiltration Test Results.....	36
Evidence for Bark Water Uptake in Reed Bigleaf Maple	38
Evidence for Bark Water Uptake in Douglas-fir	40
Evidence for Bark Water Uptake in Coast Redwood	43
Conductivity Differences by Tree Species	46
Chapter 5: Discussion	49

Chapter 6: A Broader Context	51
Appendix A: Glossary of Terms	53
Appendix B: Supplemental Information	59
Non-Significant Increases in Conductivity Following Soaking Treatment in Sandy Bigleaf Maple	59
Conductivity Differences in Reed and Sandy Bigleaf Maples	61
References	65

List of Figures

Figure 1.1. Map of the Pacific Northwest.....	4
Figure 1.2. Coast Redwood.....	6
Figure 1.3. Douglas-fir.....	7
Figure 1.4. Bigleaf Maple.....	7
Figure 1.5. Epiphytes.....	10
Figure 1.6. Cladogram of land plants.....	10
Figure 2.1. Tracheids and vessel elements.....	16
Figure 2.2. Diagram of water moment in a vascular plant.....	20
Figure 2.3. Embolism and air seeding in xylem vessels.....	22
Figure 3.1. Diagram of a Sperry apparatus.....	29
Figure 3.2. Flowcharts of centrifugation and drydown methods.....	32
Figure 4.1. Epiphyte dry mass on Bigleaf Maple by site.....	35
Figure 4.2. Branch age of Bigleaf Maple by site.....	36
Figure 4.3. Dye infiltration test.....	37
Figure 4.4. K_s and PLC of Reed Bigleaf Maple.....	39
Figure 4.5. PLC difference in Reed Bigleaf Maple.....	40
Figure 4.6. Douglas-fir water potential prior to $K_{s,min}$ measurement.....	41
Figure 4.7. K_s and PLC of Douglas-fir.....	42
Figure 4.8. PLC difference in Douglas-fir.....	43
Figure 4.9. K_s and PLC of Coast Redwood.....	45
Figure 4.10. PLC difference in Coast Redwood.....	46
Figure 4.11. PLC difference in Reed trees by species and treatment.....	48

Figure B.1. K_s and PLC of Sandy Bigleaf Maple.	60
Figure B.2. PLC difference in Sandy Bigleaf Maple.....	61
Figure B.3. K_s differences in Bigleaf Maple by site and treatment.	62
Figure B.4. PLC difference in Bigleaf Maple by site and treatment.	63

Abstract

Water moves upward from the roots through the xylem of a tree because of the negative water potential gradient that forms when water evaporates from the leaves during photosynthesis. The taller the tree, the more negative crown water potentials must be in order for water transport to still occur, effectively drought stressing the crowns of the tallest trees. However, a 2015 study on Coast Redwood suggests that these trees may be able to mitigate drought stress by absorbing water through the bark of upper canopy branches. It is unknown if bark water absorption occurs in other tree species, or if the presence of epiphytic mosses and lichens can serve to mediate this process. I investigated bark water absorption in three species of trees: Coast Redwood, to confirm the results of the previous study; Douglas-fir, because of its height, ubiquity, and economic importance; and Bigleaf Maple, because of its unusually high epiphyte loads. Xylem hydraulic conductivity (K_s) was directly measured on stems experiencing simulated drought conditions. The stems were then soaked in deionized water to test if bark water transport could reduce drought stress. Significant ($P < 0.05$) increases in hydraulic function were seen in soaked stems compared to negative controls in all three species: Bigleaf Maple (20.9 percent increase in conductivity), Douglas-fir (15.7 percent increase in conductivity), and Coast Redwood (57.3 percent increase in conductivity). This suggests that the bark of many species of trees may not be as hydrophobic as previously thought, and that refilling of embolized vessels from water absorbed through the bark is possible; however, further testing is required to verify these results.

*This thesis is
dedicated
to the trees.*

Chapter 1: The Climate and Forests of the Pacific Northwest

Mediterranean Climates and the Conifer-Dominated Forests of the Pacific Northwest

The Pacific Northwest runs along the west coast of North America from northwestern California up to the southwestern coast of Alaska. Bordered to the east by the Coast and Cascade mountain ranges, and to the west by the Pacific Ocean, this region has a unique climate that is responsible for the dense conifer-dominated forests that cover its landscapes.¹ Oceanic moderation causes a much milder climate than would otherwise be expected at these latitudes, and the high moisture content of the air masses moving inland from the Pacific Ocean is responsible for the abundant winter rainfall in this region.² The summers, however, tend to be warm and relatively dry due to the seasonal presence of offshore subtropical high-pressure regions.³ This is known as a Mediterranean-type climate.

Mediterranean climates, which are found on the western edges of continents at mid-latitudes, are characterized by a unique pattern of seasonality: hot, dry summers and cool, wet winters.^{4,5} The majority of the precipitation falls outside of the summer growing season, long periods of freezing temperatures are rare, and during the summers, the warm temperatures combined with dry air result in significant evaporation from leaf surfaces; essentially, all plants that grow in these regions must adapt to deal with seasonal drought. In many Mediterranean climates, this results in shrub-dominated ecosystems, such as the chaparral communities that flourish along much of the California coast.⁵ The Pacific Northwest follows the seasonality pattern of Mediterranean climates, but regions much further north than southern Oregon are at latitudes too high to be generally considered “true” Mediterranean climates; because of this, I will be referring to the Pacific Northwest as a Mediterranean-*type* climate.⁴ The high winter rainfall of the Pacific Northwest means that much larger trees and denser forests can be supported than in true Mediterranean climates.

Conifers differ from angiosperms (flowering plants) in important physiological aspects. Conifer needles or scales lose water at much lower rates than do the broad leaves of most angiosperms.¹ Narrower water-conducting vessels in conifers make water transport slower, but also make conifers less susceptible to the formation of air emboli in these vessels in very dry or cold conditions (see Chapter 2 for more details on vessel structure and embolism formation).⁶ Resistance to freeze-thaw embolism is why coniferous forests tend to dominate in subarctic latitudes and at high elevations. Angiosperms, particularly deciduous species, fare better in warmer, damper climates with long growing seasons and can out-compete conifers in these conditions. In many temperate regions at similar latitudes to the Pacific Northwest, deciduous angiosperms dominate forests. However, in the Pacific Northwest, the lack of precipitation during the growing season favors conifers over angiosperms, resulting in the evergreen conifer-dominated, high-biomass forests of the Pacific Northwest.¹

Despite the challenges that seasonal drought places on trees, the mild, Mediterranean-type climates of the Pacific Northwest are home to some of the tallest trees in the world, especially along the coast. The tallest trees face many challenges related to water movement because of their height (see Chapter 2) and therefore can only reach prodigious heights in the most favorable conditions. Mild winters with temperatures that rarely dip below freezing for extended periods of time except at high elevations reduce the risk of freeze-thaw embolism (see Chapter 2).⁷ The foggy summers along the coast mitigate some of the effects of seasonal drought; several species of trees native to the northern California coast, including Douglas-fir (*Pseudotsuga menziesii* var. *menziesii*) and Coast Redwood (*Sequoia sempervirens*), are known to be capable of absorbing water through their leaves, a useful adaptation in a climate where fog dampens canopies but rain is uncommon for much of the year.⁸

The mountain ranges of northern California, Oregon, and Washington play an important role in shaping the climate of the Pacific Northwest. As wet air masses move inland off the Pacific Ocean, the steep slopes of the Coast Range (or, in northern Washington, the Olympic Mountains) forces them to rise, cool, and condense, producing extremely high winter rainfall as well as abundant summer fog along the coast and the western slopes of these mountains.² The wet forests along the Pacific coast are dominated

by Sitka Spruce (*Picea sitchensis*), Western Hemlock (*Tsuga heterophylla*), and Douglas-fir and are some of the most productive forests in the world in terms of biomass produced per acre.⁹ In pockets of the northern California coast, where there are on average, more densely foggy days per year than anywhere else in the United States, Coast Redwood also grows as a dominant species.¹⁰ The Olympic Peninsula of western Washington receives the highest rainfall in the continental United States, resulting in incredibly lush temperate rainforests with exceptionally high amounts of epiphyte biomass.^{11,12} The Columbia River Gorge, which carves through both the Cascades and the Coast Range, allows moist, mild coastal air to penetrate much deeper inland than would otherwise be possible.²

Regions of northern California east of the Coast Range are not generally considered part of the Pacific Northwest. East of the Coast Range in Oregon is the Willamette Valley, which runs north-south along most of the state. Here lie Portland, Salem, Eugene, and much of Oregon's agricultural land. The valley is drier than the Coast Range, with relatively little summer rainfall.² Historically, the valley was dominated by Oregon White Oak (*Quercus garryana*) savannah, although less than five percent of this ecosystem remains today, much of it now replaced by Douglas-fir, which thrives in the absence of regular wildfires.¹³ The Puget Sound basin in Washington sits between the Coast and Cascade mountains in Washington and is cooler than the Willamette Valley, with less dry summers due to the higher latitudes and proximity to the marine air of Puget Sound. Snow is more common here than in the Willamette Valley.¹¹

East again from the Willamette Valley and the Puget Sound basin are the Cascade Mountains. Extending all the way to central British Columbia from their southernmost peak in Northern California, the Cascades are mainly volcanic in origin, the result of the subduction of the Juan de Fuca plate under the North American Plate.¹⁴ They rise majestically to an average height of about 5000 feet, with some isolated peaks more than double that.² Mount Hood, due east of Portland, is the highest point in Oregon, at 11,239 feet above sea level, but Mount Rainier (14,408 feet) in Washington and Mount Shasta (14,180 feet) in California are much taller.² Just as in the Coast Ranges, the sudden protrusion of the Cascades forces east-moving air masses to rise and cool as they pass over the mountains. Consequently, the rainfall on the west slope of the Cascades is also very high, although less than that of the Olympic Mountains or Coast Range.^{2,11} The

lower-elevation west slopes of the Cascades are dominated by lush, mixed-coniferous forests of Douglas-fir (*Pseudotsuga menziesii*), Western Red Cedar (*Thuja plicata*), Western Hemlock, and several species of true firs (*Abies* spp.).¹⁵ Deciduous species are less dominant, but Red Alder (*Alnus rubra*) and Black Cottonwood (*Populus trichocarpa*) are common in riparian areas, and Bigleaf Maple (*Acer macrophyllum*) can be found in scattered groves throughout these forests.¹⁶ Epiphytic mosses and lichens are abundant, although generally not as much as along the coast.¹⁶

East of the Cascades is not considered to be a part of the Pacific Northwest. It is much drier than the west side, since very little moisture remains in the east-moving air masses that cross the Cascade crest.² The vegetation is a mixture of shrubs, grasses, and dry Ponderosa Pine (*Pinus ponderosa*) forests.¹⁷

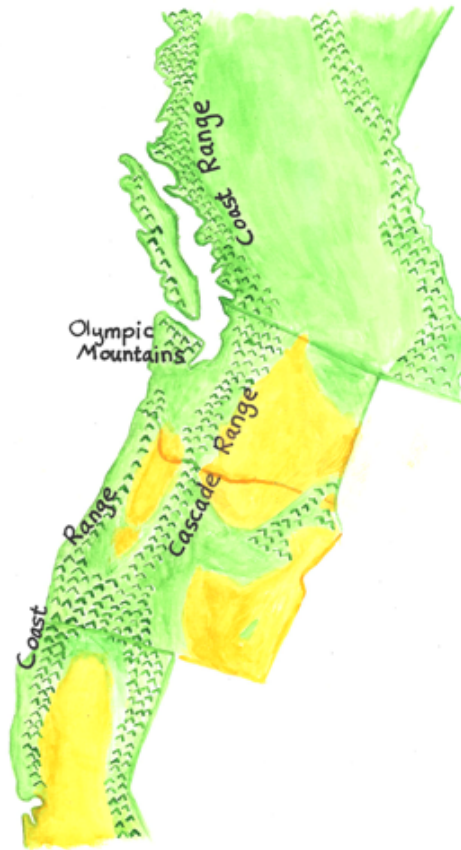


Figure 1.1. Map of the Pacific Northwest.

This map shows the major mountain ranges of the central region of the Pacific Northwest (not including northern British Columbia or Alaska) as well as the general vegetation of the region: green represents forested areas, yellow represents unforested areas (mainly grasslands and agricultural land).

Coast Redwood, Douglas-fir, Bigleaf Maple, and Epiphytes

Endemic to the “fog belt” of the northern California coast, Coast Redwoods (*Sequoia sempervirens* (D. Don) Endl.) are members of the cedar family (Cupressaceae) and are the tallest living trees on earth, reaching nearly 116 meters in height. Their immense height has piqued the interest of many people, both scientists and not; nearly 1.5 million people visited Redwood National Park in northwestern California in 2015.¹⁸ Because of this, Coast Redwood is a relatively well-studied species, with numerous published studies on canopy water physiology. Coast Redwood is the only tree that has been found to perform both bark and foliar water uptake (see Chapter 2), although no published studies exist on bark water uptake in other tree species. In the foggy climates that they are native to, absorption of water in bark and leaves of dampened redwood canopies may have significant impacts on reducing height-exacerbated drought stress.^{8,19}

Unlike Coast Redwood, which has a narrow range along the northern California coast, Coastal Douglas-fir (*Pseudotsuga menziesii* (Mirb.) Franco var. *menziesii*), referred to in this thesis and elsewhere as simply “Douglas-fir,” is a member of the pine family (Pinaceae) and is widespread across the Pacific Northwest; another variant of the species, Rocky Mountain Douglas-fir (*Pseudotsuga menziesii* var. *glauca*), is native to the Rocky Mountains. Douglas-fir is one of the most abundant conifer species at low and mid elevations in the Pacific Northwest, and at mid elevations in California.²⁰ On the damp west slopes of the Coast, Cascade, and Olympic mountain ranges, Douglas-fir is often co-dominant with a variety of other conifer species, including Western Hemlock (*Tsuga heterophylla*), Western Red Cedar (*Thuja plicata*), and several species of true fir (*Abies* spp.).²⁰ Douglas-fir is an important forestry tree both within its native range in the Pacific Northwest, and across Britain and continental Europe, where it is widely planted for harvest.²¹ Its ubiquity and economic importance makes Douglas-fir widely studied by plant physiological ecologists. Like Coast Redwood, Douglas-fir has been shown to perform significant foliar water uptake under some conditions; however, bark water uptake has not been studied in Douglas-fir.⁸

Douglas-fir trees can live for more than 1000 years. Today, a few individuals reach heights of nearly 75 meters, although the tallest Douglas-fir ever recorded was cut

in 1897 near Forks, Washington and measured 142 meters tall — far taller than the tallest Coast Redwood alive today.²² In the damper portions of their range, old-growth Douglas-fir forests can host prodigious epiphytic moss and lichen communities.²³



Figure 1.2. Coast Redwood.

Coast Redwoods can be identified by the combination of their needles, which lie in a flat plane, unlike those of most members of Pinaceae, and their cones, which are small and relatively open compared with those of most other conifers. Coast Redwoods, particularly older and larger trees, tend to exhibit a fairly uneven branching pattern compared with other conifers like Douglas-fir. Map shows the native range of Coast Redwood (red).



Figure 1.3. Douglas-fir

Pointed buds on the tips of branches and cones with protruding bracts behind each scale help identify Douglas-fir, which otherwise is easily confused with the true firs; rounded needles distinguish it from spruces. Range map shows the native range of Coastal Douglas-fir (*P. menziesii* var. *menziesii*) (red), as well as that of Rocky Mountain Douglas-fir (*P. menziesii* var. *glauca*) (blue).



Figure 1.4. Bigleaf Maple.

Bigleaf Maple tree depicted in winter for better view of bark; green on trunk and large branches is due to epiphytic moss coverage. In the absence of epiphytes, bark is light brown and ridged. Map shows the native range of Bigleaf Maple (red).

Bigleaf Maple (*Acer macrophyllum* Pursh) is a member of the maple family (Aceraceae) native to the Pacific Northwest.²⁴ Bigleaf Maple trees are relatively large angiosperms (flowering plants) for the region, generally reaching 15–30 m in height.¹⁶ They can be found in many diverse forest types, including as a dominant overstory species on rocky, montaine slopes in the Washington and Oregon Coast Ranges, as well as in scattered groves in old growth Sitka Spruce-dominated temperate rainforests on Washington's Olympic Peninsula.²⁴ They are also commonly planted in gardens and yards in cities like Portland, Oregon. In northwestern Oregon, Bigleaf Maple is often found growing naturally in mixed, conifer-dominated forests.

Bigleaf Maple trees tend to have unusually high epiphyte loads compared to the conifer species that they co-occur with. In the temperate rainforests of western Washington's Olympic Peninsula, the average dry mass of epiphytes on a single old-growth Bigleaf Maple tree is 35.5 kg, covering an average per-tree surface area of 30.56 m², and the estimated epiphyte biomass of a single-species old-growth Bigleaf Maple forest on the Olympic Peninsula is 6870 kg/hectare, well within the range described for tropical rainforests.¹² It has been theorized that the unusually high epiphyte density on Bigleaf Maples is due to differences in bark chemistry between maples and the dominant conifer species in these forests.²⁵ Regardless of the cause, the high epiphyte coverage has made Bigleaf Maple the tree of choice for several studies on epiphyte diversity and biomass in temperate forests.

Epiphytes are species of plants and lichens that grow on other plants for the purpose of physical support; they are non-parasitic. Although epiphytes can come from a wide range of taxonomic divisions, this thesis focuses on the water-holding capabilities of epiphytes, so I will be primarily discussing epiphytic bryophytes (mosses and liverworts) and lichens, which are often capable of holding a great deal of water — some species can reach between 300 and 3000 percent of their dry mass when fully saturated.²⁶ Although the greatest epiphyte diversity is found in tropical rainforests, where the warm, humid climate is particularly conducive to their growth, much of the Pacific Northwest also enjoys abundant epiphytes due to the relatively wet, mild climate.¹²

Species morphologically similar to the bryophytes of today were some of the first land plants, about 300 million years ago.^{27,28} Bryophytes are seedless (spore-producing),

non-vascular plants. They do not have roots and therefore cannot absorb water and nutrients from the ground as vascular plants do.²⁹ Lichens, on the other hand, are not plants. They are symbionts, composed of an alga and/or cyanobacterium species living in association with one or more fungal species.³⁰ The alga or cyanobacterium provides the fungus with carbon via photosynthesis, while the fungus keeps the lichen attached to the substrate and provides a large surface area for gas exchange, photosynthesis, and hydration to take place.³⁰ Densely packed fungal hyphae make up the surface of the lichen and contain polysaccharides that are highly water absorbant.³⁰ Both bryophytes and lichens do not possess true roots or a vascular system and thus cannot uptake metabolically significant quantities of water from the soil; instead they rely on water and nutrients absorbed from air or rainwater.²⁸ This absorption is facilitated by high surface area to volume ratios and lack of the water-repellent cuticle that reduces evaporative water loss in higher plants. The flip side of this is that the qualities that increase atmospheric water and nutrient absorption also leave many species of bryophytes and lichens are very sensitive to air pollution, which is why urban sites tend to have less epiphytic biomass than rural sites.³¹

Understanding the physiological effects of the presence or absence of epiphytes could well be a crucial part of understanding the water and nutrient dynamics of forests in the Pacific Northwest. Branches covered in epiphytes are known to collect and hold much more water and nutrients than smooth branches, simply by virtue of the additional surface area provided by the epiphytes.¹² The long-term water-holding capacity of many epiphyte masses is prodigious, too: even after week-long dry periods, epiphytes remain damp.¹²



Figure 1.5. Epiphytes.

The author holds *Selaginella oregana*, a mosslike vascular plant known as a club moss that grows as an epiphyte in the Pacific Northwest, up to her face. The large tree in the background is a Bigleaf Maple; note the ferns, *S. oregana*, and mosses covering the trunk and branches. Photo taken in the Hoh Rainforest, Washington, by Loralee Bandy.

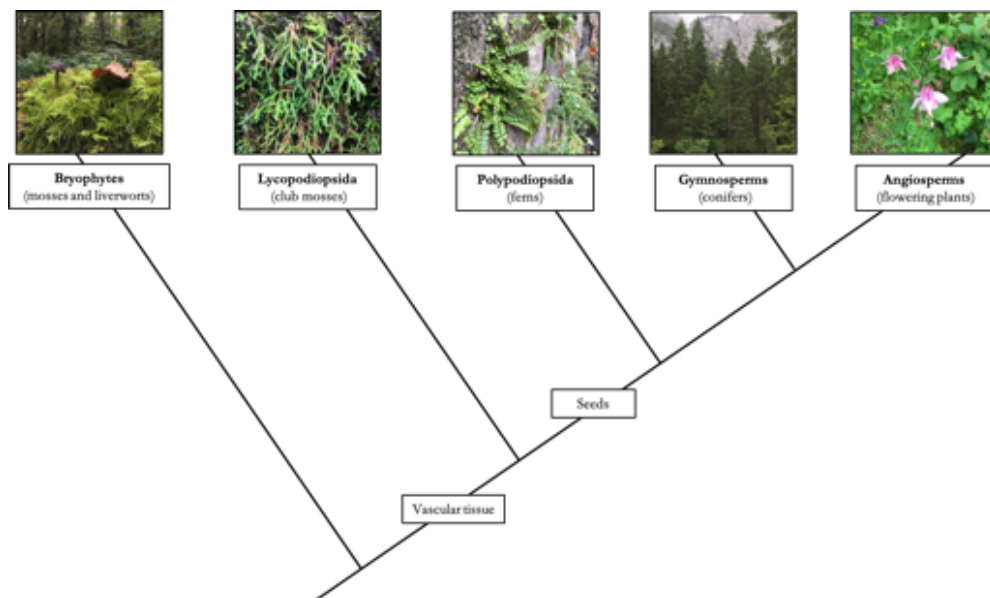


Figure 1.6. Cladogram of land plants.

This cladogram shows how land plants are broadly related; the further left two branches of the cladogram diverge, the longer ago the groups shared a common ancestor. Based on a US Forest Service cladogram.³² Photo for Lycopodiopsida courtesy of iNaturalist.

Climate Change and the Role of Hotter Drought

The Earth's climate is not a static thing. In the approximately 4.5 billion years that the Earth has existed for, it has undergone many, many cycles of warming and cooling. Large-scale temperature fluctuations can occur for three main reasons: changes in the amount of solar radiation received from the Sun, the reflectivity of the Earth, or changes in how the heat captured by our atmosphere is lost to space.³³ Monitoring of solar output has determined that changes in the amount of solar radiation received by the earth has not changed enough to be responsible for the major increases in global temperatures over the past 30 years.³³ Climate research unanimously agrees: the current warming trend is due to increased greenhouse gas emissions.

The Earth's lower atmosphere is made up primarily (78 percent) of nitrogen (N_2), an inert, unreactive gas. Oxygen (O_2) accounts for 21 percent of the atmosphere, and the noble gas Argon (Ar) another 0.9 percent.⁵ None of these gases are considered "greenhouse gases;" that is, due to their chemical structure, they are very ineffective at trapping the infrared heat produced by the Sun. The remaining tenth of a percent of the atmosphere includes nearly all of the greenhouse gases responsible for trapping heat on Earth.³⁴

What makes a gas a greenhouse gas? Gases are considered greenhouse gases if they can absorb infrared radiation. Only certain molecules can do so. A gas molecule must be made up of three or more atoms in order to absorb infrared radiation and act as a greenhouse gas. When struck by an infrared photon of a certain wavelength, a greenhouse gas molecule will begin to vibrate, its molecular bonds stretching and bending. When this vibrating molecule collides with other gas molecules in the atmosphere, it transfers some of its vibrational energy to them, and they begin to move faster. This faster molecular movement is what we perceive as heat. Depending on its molecular structure, a greenhouse gas can absorb different wavelengths of solar infrared radiation, which is why the same amounts of different greenhouse gases can have drastically different impacts on the climate.³⁵

Carbon dioxide is probably the most well-known greenhouse gas. The product of any combustion reaction (including metabolic processes), its atmospheric levels have greatly increased in the industrial era. In 2013, the carbon dioxide concentration in the

atmosphere rose above 400 ppm for the first time in the last million years.³⁶ The human production of carbon dioxide alone accounts for approximately 63 percent of the global temperature increase attributed to anthropogenic (human-caused) greenhouse gas emissions.³³ The other 37 percent is attributable to anthropogenic production of other, much more potent greenhouse gases, the most common of which include methane (CH₄), ozone (O₃), chlorofluorocarbons, and nitrous oxide (N₂O).³³

Oregon in particular has already seen significant warming. The mean July temperature in the state has increased by between 1 and 2 degrees Fahrenheit in each of the last three decades.³⁷ Climate models suggest that Oregon will continue to warm through at least the next century. The extent to which this warming will occur is based, of course, on the extent to which greenhouse gas emissions can be reduced. If emissions can be substantially reduced (a best-case scenario), the mean temperature in the Pacific Northwest is predicted to increase from the 1950–2005 mean by about 6° C by 2100. If emissions increase substantially over the next century, that increase might be closer to 11° C.³³

The impact that these temperature increases will have on the people and wildlife of the Pacific Northwest has a lot to do with when and where the temperatures will increase, as well as with how precipitation patterns are predicted to change. Higher temperatures in the winter, for example, could have profoundly different effects than those in the summer. Several climate models suggest that temperatures will increase the most in the summer.³³ Events of extreme heat will likely be more common, while those of extreme cold will become less common. The annual amount of freeze-free days is predicted to increase by an average of 35 days for the Pacific Northwest for the 2041–2070 mean compared to the measured 1971–2000 mean.³³

The amount and pattern of precipitation events in the Pacific Northwest is also predicted to be affected significantly by climate change. Although total average precipitation over the region is not predicted to be greatly affected (models suggest an average of 3–5 percent increase in annual precipitation), summer precipitation — already low — is projected to decrease by as much as 30 percent by the year 2100.³³ With rising temperatures, the type of precipitation will also change. The ratio of rain to snow will probably increase in most — if not all — regions.³³ Mountain snowpack will likely

decrease significantly, which may have severe impacts on the amount of water available for agricultural, personal, and recreational uses.

Forests cover 49 percent of Oregon and 52 percent of Washington.³³ Because of the Mediterranean-type climate in the Pacific Northwest, over 75 percent of the precipitation currently occurs outside of the growing season, causing water availability to often be the limiting factor in summer vegetation growth.³³ The climate models discussed above strongly suggest that these already-existing summer water deficits will only increase in the future.³³ This will inevitably have serious impacts on forest (and other plant) health in the future. Plants move water up from their roots to their leaves, where it is evaporated during photosynthetic gas exchange (see Chapter 2) through a process known as transpiration. In hotter or drier conditions, the transpiration rate is increased and plants dry out faster. Under climate change, transpiration rates will increase across the Pacific Northwest, particularly in the already water-limited, hot summers.³³

Chapter 2: Plant Hydraulics and the Tall-Tree Problem

The Biophysics of Water in Plants

Water is a small, highly polar molecule, which enables it to form strong hydrogen bonds with itself (cohesion) as well as hydrogen bonds with other polar surfaces (adhesion).⁷ The propensity of water to form these strong hydrogen bonds is the main reason for many of the unique, physiologically important properties of water.⁷ It has an unusually high specific heat capacity (energy required to increase the temperature of the substance by a specific amount) that helps buffer temperature fluctuations; this is why coastal regions experience much more minimal seasonal and diurnal temperature variability than do inland regions.⁷ Water also has the highest value of the latent heat of vaporization of any liquid for the same reason. Latent heat of vaporization is the amount of energy needed to separate molecules from the liquid phase and turn them into gas phase.⁷ This is important in plant physiology because the high amount of energy it takes to evaporate water results in cooling of the surfaces (such as leaves) from which water has evaporated.

Hydrogen bonding also gives water a high tensile strength.⁷ Tensile strength is the maximum force per unit area that a continuous column of water can withstand before breaking.⁷ Pure, degassed water can resist pressures more negative than -20 MPa, although this value is unrealistic for natural water columns due to the inevitable presence of microscopic gas bubbles that expand when placed under negative pressure.⁷

All vascular plants possess an interconnected network of non-living, hollow cells that serve to transport water throughout the plant.³⁸ This is known as the xylem. The water-conducting cells are called tracheary elements. Tracheary elements are dead cells with a developed secondary wall, an inner cell wall that conveys additional structural support.⁷ Functional, water-conducting xylem cells are dead because water movement through dead cells requires a smaller pressure gradient than movement through living cells, since it does not require water to cross plasma membranes. However, there is still

considerable resistance created by the xylem.⁷ There are two main types of tracheary elements: tracheids and vessel elements (see Figure 2.1).

Tracheids are present in all vascular plants. They are elongated, spindle-shaped cells packed together vertically in the xylem tissue.⁷ The cells are covered in pits — microscopic holes in the secondary wall. Pit pairs — pits opposite to one another in adjacent cells — allow water movement between adjacent tracheids with minimal resistance.⁷ The water-permeable membrane between pit pairs is known as the pit membrane and consists of the primary cell walls of the two adjacent cells and the middle lamella (membrane).⁷ Conifer tracheids have pit membranes with a central thickened region (torus) surrounded by a porous, flexible margo where the water moves through. The torus acts as a valve to control water movement through the pit pairs.⁷ This prevents air emboli from travelling between neighboring tracheids.⁷ Non-conifer plants do not have tori, and instead have generally smaller pit membranes to reduce embolism movement.⁷

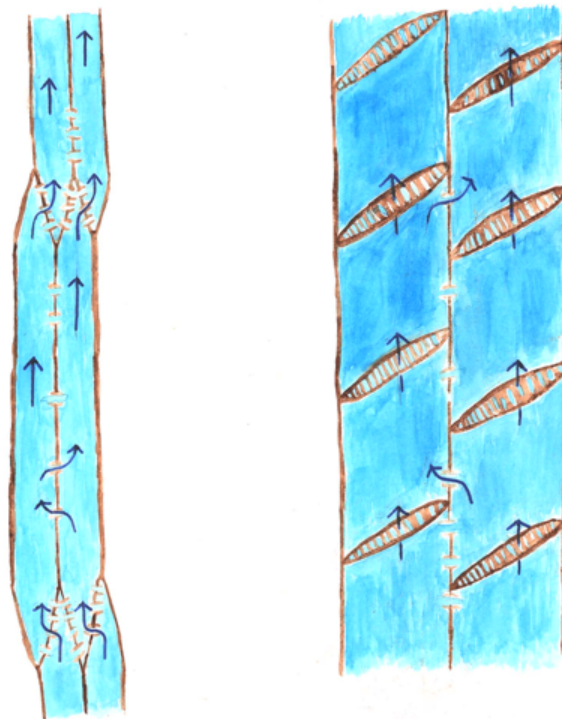


Figure 2.1. Tracheids and vessel elements.

Tracheids (left) are long, thin cells. Note the water moving between cells through the adjoining pit pairs. Vessel elements (right) are shorter, wider cells that are stacked to form long vessels; the majority of water moves through the perforated end plates.

Vessel elements have only been found in angiosperms, some ferns, and the Gnetales, a small group of non-coniferous gymnosperms.⁷ They are generally shorter and wider cells than tracheids.⁷ Although they also contain pits, the main defining feature of vessel elements is the perforated ends of the cells that allow them to be stacked vertically to form long vessels, the length of which vary widely from species to species.⁷

Water potential (Ψ_w) is the driving force behind water movement in plants and is essential to understand for plant physiology.⁷ To understand water potential, however, we must first understand the concept of chemical potential, “a quantitative expression of the free energy associated with a substance. In thermodynamics, free energy represents the potential for performing work,” where work is defined as force times distance.⁷ Free energy is associated with the entropy (disorder) of a system: a more ordered system has greater free energy (and thus greater chemical potential).⁷ Things proceed spontaneously — without an input of energy — from regions of higher chemical potential to ones of lower chemical potential. The chemical potential of water therefore represents the free energy associated with water.⁷ Water flows spontaneously from regions of higher chemical potential to ones of lower chemical potential.⁷

Water potential is defined as the chemical potential of water divided by the volume of one mole of water; the unit of water potential is thus measured in (free) energy per unit volume (J m^{-3}), which is equivalent to units of pressure (such as MPa), which are often used to measure water potential.⁷ Water enters and exits plant cells along a water potential gradient, moving from an area of high water potential to one of lower water potential.⁷ The relative water potential between adjacent plant cells is therefore much more important than the absolute water potential; however, if desired, the absolute water potential in a living cell or xylem tissue can be calculated using the equation:

$$\Psi_w = \Psi_s + \Psi_p + \Psi_g$$

Where Ψ_s is the solute potential, Ψ_p is the pressure potential of the solution, and Ψ_g is the effect of gravity on the water potential.⁷

The solute potential represents the combined effects of any and all dissolved solutes on water potential.⁷ Because the presence of solutes reduces water’s free energy (and thus water potential) by increasing the entropy of the system, greater solute concentrations result in decreased water potential.⁷ The solute potential of dilute (less

than 0.1 mol/L) solutions is given by the equation $\Psi_s = -RTc$ where R is the gas constant, T is the temperature in degrees Kelvin, and c is the total solute concentration of the solution.⁷ Plants can adjust the solute concentration of their cells in order to adjust their relative water potentials, with higher solute concentrations helping plant cells maintain turgor in dry conditions.⁷

The pressure potential is measured as a deviation from atmospheric pressure.⁷ In the xylem of plant tissues, negative pressures potentials develop from the force of the water column being pulled upward by leaf transpiration.⁷ However, on a cellular level pressure potentials are positive, indicating water pushing out at the cell walls; this is known as turgor pressure.⁷ Turgor pressure is essential for many plant physiological processes as well as to keep non-woody tissues rigid.⁷

The downward force of gravity also has a significant effect on water potential at the xylem level, although a negligible effect on water potential on a cellular level.⁷ The pressure due to gravity can be described by the equation $\Psi_g = \rho_w gh$, where ρ_w is the density of water and g is the acceleration due to gravity. $\rho_w g$ is equal to 0.01 MPa m⁻¹, so a vertical distance of 10 m translates into a 0.1 MPa change in water potential.⁷

Water Movement in Plants and the Cohesion-Tension Theory

Water is often one of the most limiting resources for land plants in nature.⁷ Plants use large amounts of water compared with other organisms because photosynthesis on land requires that CO₂ uptake is coupled with water loss through the stomatal gas exchange pathway.⁷ Up to 400 water molecules may be lost for every CO₂ molecule gained because of the relative concentration gradients; air is generally very dry and contains very little CO₂.⁷ This results in very high water loss: about 97 percent of the water that is absorbed by roots is lost to evaporation off the leaf surface (transpiration) and is never used metabolically.⁷ Only about 3 percent is used to supply growth or in metabolic processes.⁷

During transpiration, water is pulled from the xylem into the cell walls of the mesophyll and then evaporates into the air spaces of the leaf, exiting the leaf through the

stomata (pores). Very little water is lost through the hydrophobic waxy cuticle of vascular plants; only an estimated 5 percent of the water lost from leaves escapes through the cuticle.⁷ The vast majority of water is lost through the stomata during gas exchange. Movement of liquid water through the xylem is controlled by water potential gradients, but movement of water vapor is controlled by diffusion; the final part of transpiration is driven by the concentration gradient of water vapor.⁷ The leaf has a high concentration of water vapor relative to the air, so the leaf loses water. This difference in water vapor concentration is expressed as $c_{wv(\text{leaf})} - c_{wv(\text{air})}$.⁷ The rate of transpiration also depends on the diffusion resistance of the evaporation pathway, which consists of two components: resistance associated with diffusion through stomatal pore, and resistance due to the boundary layer of the leaf (the layer of still area created by the physical shape of the leaf).⁷ The thickness of this boundary layer depends on wind speed and leaf size, with higher winds and smaller leaves corresponding to faster transpiration.⁷ The stomatal pore provides a low resistance pathway for gas exchange. Stomata are open in the day for photosynthesis and closed at night when water is not a limiting factor, but when it is, stomata may close partially or totally even in sunny conditions.⁷ Stomatal opening is controlled by guard cells, which surround the stomatal pore and allow for control of opening and closing based on environmental conditions.⁷ Guard cells of dicots are elliptical (kidney shaped) with a central pore. They are differentially thickened with very thick inner and outer walls and thin wall in contact with epidermis, and a medium thick pore wall. When the guard cell increases in volume, the weaker outer wall bows outward, opening the pore.⁷ Guard cell turgor pressure is therefore the regulator for stomatal opening. Turgor pressure in these cells is regulated by things such as light intensity, leaf water status, and intracellular CO₂ concentrations. Ions are uptaken by the guard cells in response to favorable conditions for photosynthesis, increasing their turgor pressure when water flows along its water potential gradient.⁷

Leaf transpiration is the essential driving force for water movement in plants. During transpiration, as water evaporates out of the leaves, some water is pulled through to the cellular interstices (area between the cells), forming curved air-water interfaces due to water's surface tension, inducing tension — a negative pressure in the xylem water column.⁷ The tension is transmitted throughout the entire water column of the plant

because of water's tendency to form strong hydrogen bonds with itself (i.e., cohesion). This creates a pressure gradient, with the highest pressures in the roots and the lowest in the leaves, ultimately resulting in the uptake of soil water from the roots to replace that water lost to leaf evaporation.³⁹ The greater the rate of leaf water evaporation, the more curved the air-water interfaces become and thus the greater the tension in the water column. This is known as the Cohesion-Tension Theory of plant water transport, first proposed in 1894 by Dixon and Joly.³⁹

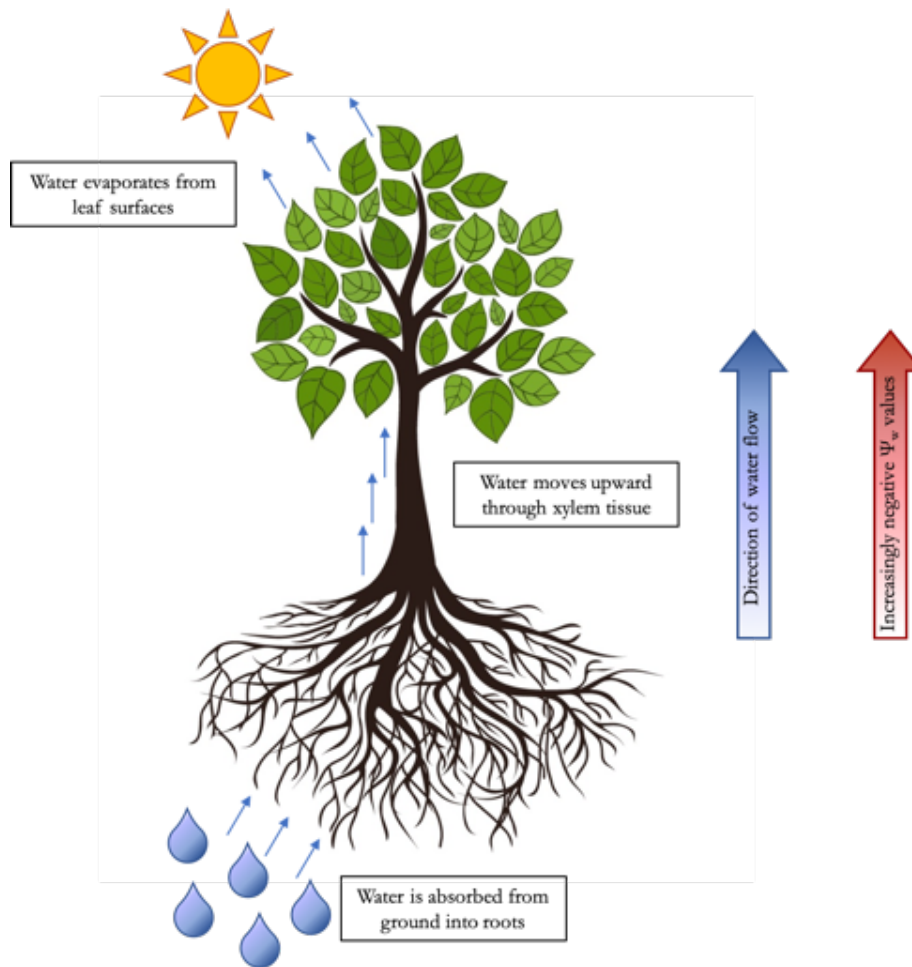


Figure 2.2. Diagram of water movement in a vascular plant.

Water is first absorbed from damp soil into roots, which have a more negative water potential than the surrounding soil. The water then moves upwards through the xylem along a gradient of increasingly negative water potentials until it evaporates off leaf surfaces.

There are physiological challenges associated with the development of the kind of high tensions associated with the xylems of taller trees.⁷ For a very tall tree (100 m), the effects of the xylem frictional resistance combined with those of gravity requires that the pressure difference between the top and bottom of the tree be at least 2.0 MPa in order for water transport to occur.⁷ Water under tension transmits that force to the xylem walls; if they are too weak, they could collapse; because of this, plants that experience high xylem tensions tend to have denser wood.^{7,40} Tall trees, even those growing in relatively damp environments such as the Pacific Northwest, tend to experience some of the xylem tension-related challenges otherwise associated with drought. This leads us to what we will call the tall-tree problem, which is discussed later on in this chapter.

Xylem Embolism, Measurement of Cavitation, and Embolism Repair

The water column of a plant is almost never totally unbroken. The high force of the negative pressure pulling upward on the water in the xylem can lead to the formation of air bubbles — emboli — in the water column.³⁹ The semi-porous xylem walls cannot prevent air from being sucked into the vessels if the water column is under very high pressure — such as when the plant is under significant drought stress, or close to the top of a very tall tree.³⁹

Water in the xylem is in a physically metastable state: it is under enough tension that it should spontaneously vaporize but it remains in the liquid state due to cohesion and adhesion, as well as the structure of the xylem itself minimizing the possibility of nucleation sites (sites that lower the energy barrier separating the gas and liquid phases).⁷ Gas bubbles are the most significant nucleation sites, and they expand when the surface tension is not enough to cancel out the water column tension.⁷ Once a bubble begins to expand, it reduces the curvature of the air water interface even more, making it easier for it to expand further. A bubble that exceeds the critical size for expansion will quickly expand to fill the entire conduit.⁷ Pit membranes prevent many bubbles from spreading between tracheids or vessel elements, but can also serve as entry sites for air when one site is totally exposed to air (due to damage or an adjacent embolized cell); air enters

when the pressure difference across the membrane is high enough to overcome the surface tension, or to dislodge the torus in conifers (air seeding).⁷ Freezing of xylem tissues also provides a way for bubbles to form, because any dissolved gasses present in the water come out of solution when it freezes, and when the water later thaws, these bubbles do not go back into solution readily, forming air pockets.⁷

An expanded bubble (air embolism) in a tracheid or vessel element essentially destroys the conductive capabilities of that particular cell. The broken water column in that vessel cannot be pulled upward by the force of evaporation, and so ceases to conduct water.^{7,39} Luckily, emboli do not spread far because it is difficult for the expanding gas to pass through the tiny pit membranes.⁷ Although embolism reduces hydraulic function, it will not fully stop it unless severe cavitation occurs because water can “detour” around the embolized vessel or vessels by travelling through nearby un-embolized conduits.⁷ To reduce embolism, plants shut their stomata in particularly hot or dry conditions. Photosynthetic sugar production is therefore decreased when a plant is experiencing significant drought stress.

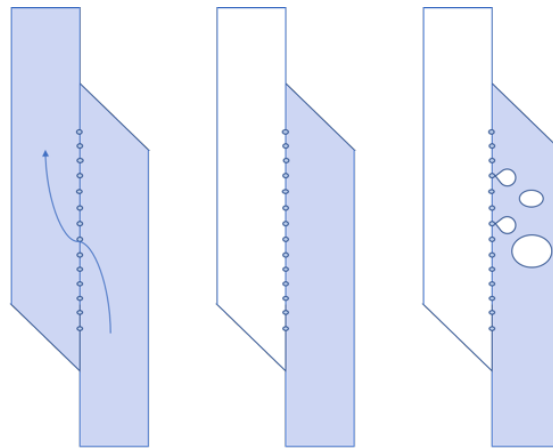


Figure 2.3. Embolism and air seeding in xylem vessels.

In the filled vessel (left), water completely fills the vessel element and flows easily up through the pit membranes (small circles between adjoining cells) along the water potential gradient. In the embolized vessel (center), however, air fills the entire vessel element and water cannot pass through the cell. In the right vessel, it is visible how the pit membranes reduce embolism spread but can still allow some air bubbles to escape into nearby vessel elements, particularly under very negative pressures (air seeding).

Based on a figure by Venturas et al. (2017).⁴¹

The water potential of xylem tissue can be measured directly in several ways, the most common of which is the pressure chamber.⁷ Pressure chambers measure water potential by applying external gas pressure to the leaf end of a cut stem until the pressure is equalized (the xylem water potential is zero); once the pressure moves slightly past this point, water will start to be forced out of the cut end of the stem and the water potential can be thus recorded.⁷

Xylem hydraulic conductivity is used to measure embolism. A Sperry apparatus is one common way of directly measuring xylem hydraulic conductivity. The hydraulic conductivity (K_h) is computed as the mass flow rate of water through the branch divided by the pressure gradient (the pressure difference between branch ends divided by branch length); this can be easily standardized to give hydraulic conductivity per unit area (stem-specific conductivity, K_s).⁴² The maximum possible hydraulic conductivity of any given branch segment can be found by placing the segment in a water bath under vacuum overnight to remove all emboli and completely fill the xylem tissue with water. This can be used to calculate the percent loss in conductivity (PLC):

$$PLC = 1 - \frac{K_h}{K_{h,max}} = 1 - \frac{K_s}{K_{s,max}}$$

Vulnerability curves quantify the resistance to cavitation of a specific species, although this can vary due to environmental factors.⁷ PLC is plotted by xylem water potential; PLC increases with increasingly negative xylem water potential. Cavitation is induced either via centrifugation, which can be calibrated to produce negative pressures at known values, or through benchtop drydown.⁴³ The shape of a vulnerability curve varies widely. More drought-adapted species tend to be less vulnerable to cavitation: they lose hydraulic function at much more negative water potentials than do less drought-adapted species.⁷

Emboli can be repaired through any of the several pathways for embolism repair. Annual new xylem growth contributes to embolism repair by replacing old cavitated vessels with new, unblocked tissue.⁷ At night, transpiration rates are low because stomata do not need to be open for photosynthesis, and the roots-to-leaves pressure gradient equilibrates; cell turgor pressure increases, which may dissolve some gas bubbles back into the water column. In small plants in very hydrated conditions, positive root pressure may be enough to redissolve bubbles.⁷

Whether embolism can be repaired where the xylem is under negative pressure is hotly debated. Some studies suggest that embolism repair under tension is indeed possible; one such study utilized high-resolution x-ray computed tomography (HRCT), which can show water movement in real time, to view refilling of embolized conduits in grapevine after irrigation.³⁸ However, it is not clear that this can translate to refilling in taller trees under more negative pressure. Methodological concerns around refilling in these contexts arise. Damage to the stem when cutting it for direct hydraulic conductivity measurement or impurities present in the excision water can trigger additional post-harvest xylem cavitation, which can lead to measurement inaccuracies.⁴¹

Canopy Water Uptake and the Tall-Tree Problem

The tallest trees face another issue when it comes to water transport: gravity. As the negative pressure created by leaf water evaporation “pulls” the xylem water column upward, gravity also pulls it downward. The taller the tree, the longer and heavier the water column is, and the greater the upward force must be in order to counteract gravity and transport water from the roots to the crown leaves. However, if the xylem pressure is too negative it will create embolism and reduce transport efficiency further. Because of this, it has been predicted that the height of any tree has an upper bound of between 122 and 130 meters — not much taller than the tallest Coast Redwoods alive today.⁴⁴ The difficulty that tall trees face in moving water will only be exacerbated as the climate changes. Taller trees have wider xylem conduits, making them generally more vulnerable to embolism formation than shorter trees of the same species.⁴⁵ As the climate of the Pacific Northwest gets warmer and drier, what will happen to the world’s tallest trees?

New research suggests that some species of trees might have other strategies to combat the tall-tree problem. Although root water movement is height limited, canopy water uptake might provide a potential solution, particularly in climates with frequent canopy wetting events like the coastal Pacific Northwest. Foliar (leaf) water uptake is the most well known form of canopy water uptake. Several plant species from a wide variety of taxa, including conifers, angiosperms, and ferns, have been observed to demonstrate the ability to absorb water through their leaves when the leaves are fully submerged,

although the specific pathway of leaf water entry in many species is unknown.⁸ Among the species in which leaf water uptake has been documented are two of the tallest trees of the Pacific Northwest, Coast Redwood and Douglas-fir.

Bark water uptake has less well studied; indeed, there is only a single published paper that explores bark water uptake in a single species. In 2016, researchers at the University of California, Davis, found that soaking redwood branch segments, with the ends sealed to prevent water from directly entering into the xylem, for 16 hours increased xylem hydraulic conductivity significantly compared with the pre-soaking conductivity of the same segments.¹⁹ They used heavy water (water molecules containing a greater percentage of the rare isotope ^{18}O) to confirm that this was indeed due to water from the soaking treatment entering the branch segments.¹⁹ However, this study has not yet produced any follow-up work and thus remains the sole foray into the capacity of trees to absorb water through their bark to reverse xylem embolism.

My thesis expands on this work. In particular, I was interested in the ecological implications of bark water uptake. Does bark water uptake occur in other tree species? Will bark water uptake help trees in the Pacific Northwest cope with the hotter, drier summers of the future? Does the presence of epiphytes affect the capacity of a branch to absorb water through the bark surfaces? I chose to confirm the results of the previous study that found evidence for embolism reversal in soaked Coast Redwood, as well as explore the potential for bark water uptake in two additional iconic species of the Pacific Northwest, Douglas-fir and Bigleaf Maple.

Chapter 3: Methods

Site Selection

For ease of access, three out of four sampling sites were chosen on the Reed College campus. Each site consisted of six trees of one species.

The Reed Bigleaf Maple site was near the west end of campus close to the Greenwood Theatre building. For sampling, I selected six mature Bigleaf Maple trees that had branches within 20 feet from the ground (accessible with pole pruner).

The Douglas-fir sampling site was also near the west end of campus, on the west side of the Performing Arts Building parking lot. I selected six mature, healthy-appearing trees with branches accessible from ground level.

The Coast Redwood sampling site was on the east end of campus, in a small grove near the Studio Arts building. I selected six trees with accessible branches; these trees appeared to be mostly younger than the Bigleaf Maple or Douglas-fir trees that I sampled, but not saplings.

The Sandy Bigleaf Maple site was located at the Diack Property near Sandy, Oregon, approximately 20 miles west of Portland. I chose six mature Bigleaf Maple trees with branches within 20 feet of the ground, all but one of which were located around a meadow near the road running through the property. The sixth tree was slightly further along the road, in an open stand of mixed conifers.

Epiphyte Massing and Branch Age Methods

Twelve Bigleaf Maple branch segments (approximately 0.8 cm diameter, 140 cm long) were collected from each site (Sandy and Reed) for the purposes of measuring hydraulic conductivity and embolism reduction post-soaking treatment (see below). The age of the youngest part of the branch segment was estimated by counting growth rings. Any epiphytes present on these branch segments were removed either when they fell off

the branch during measurement or after all measurements were complete. Epiphytes were placed in paper envelopes, dried at 68°C for 72 hours, and massed.

Dye Infiltration Methods

I used dye infiltration to verify the success of the sealing method described in Mason Earles et al. During soaking treatment, it is vital that the ends of the branches be sealed in order to prevent direct entry of water into the xylem. I sealed the ends of 6 small (0.7–0.9 cm diameter) branches collected from marked Reed Douglas-fir trees, and seven branch segments collected from both the Reed Coast Redwood and the Reed Bigleaf Maple trees. The branches were cut underwater to 12–14 cm length and the ends sliced clean with a razor. The segments were dried with a towel and sealed with waterproof silicone sealant (Momentive Performance Materials, Inc), then allowed to dry for one hour. After that hour, all but one of the sealed segments and one unsealed segment (positive control) were placed in a deionized water bath containing enough food dye to thoroughly color the water (blue dye used for Douglas-fir, red dye used for Bigleaf Maple and Redwood). Samples were left in dye bath for 24 hours undisturbed and weighted down slightly to keep the ends covered. After 24 hours, segments were rinsed briefly in plain deionized water, dried, and the sealant removed. Photographs of the branch ends were taken under a dissecting microscope (1.6x zoom) to compare the positive control, negative control (left on benchtop), and the sealed soaked branch.

Measurement of Hydraulic Conductivity

Hydraulic conductivity was measured directly using a Sperry apparatus. A Sperry apparatus relies on a hanging bag of perfusion solution (20 mM potassium chloride (KCl) in degassed deionized water) to provide a positive pressure that pushes the solution through the xylem conduits of an attached branch. The rate of solution flowing through the branch was measured using a balance; a Microsoft Excel program translated this into a standardized measurement of xylem hydraulic conductivity (K_h).

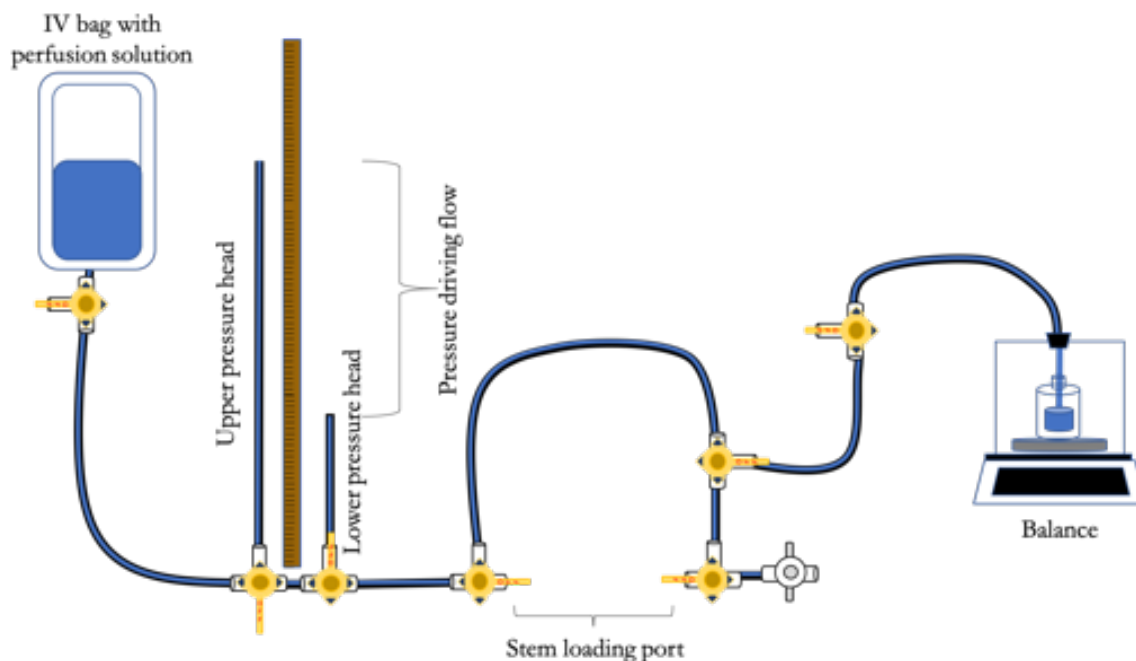


Figure 3.1. Diagram of a Sperry apparatus.

Perfusion solution flows from the IV bag through the tubing and the stem (attached in stem loading port) onto the balance; mass of solution recorded at 10-second intervals and used to calculate K_h . The difference between the upper and lower pressure heads represents the gravity-driven pressure of the solution and is used to standardize K_h .

Figure courtesy of Mark De Guzman.

Centrifugation Methods

All samples were collected the day of preparation. Branches that included segments approximately 15 cm long and 0.8 cm in diameter were cut from marked trees using either pole or hand pruners. At least 5 cm was left between the cut end of the branch and the segment used for measurement. Two branches were taken from each of the maple trees, and three were removed from each of the redwood trees. Once samples were collected, they were immediately placed in plastic garbage bags to reduce water loss. In the laboratory, the segments were excised from the whole branches underwater to reduce air embolism entry and placed in deionized water under -2.5 MPa vacuum for 10–15 hours (vacuum infiltration) to fully remove all emboli from the xylem conduits.

After vacuum infiltration, the ends of the segments were recut slightly (~1 mm) to remove any debris. The bark of the Coast Redwood stems was removed from about 5 mm from each end to facilitate sealing in the Sperry apparatus. The stems were wrapped in Parafilm to minimize leakage and the maximum xylem hydraulic conductivity ($K_{h,max}$) of each segment was measured directly using a Sperry apparatus.

After $K_{h,max}$ was measured, the stems were spun in a centrifuge (Sovall RC-5C Plus Superspeed Centrifuge) for 5 minutes. The speed of the centrifuge corresponds to a specific negative pressure; I attempted to spin samples to the P50 for each species; P50 is the negative pressure at which 50 percent of hydraulic conductivity is lost. I chose P50 because it is well within the physiological range of what trees can recover from, but high enough that the differences between $K_{h,max}$ and $K_{h,min}$ should be significant. Prior data from vulnerability curves, which plot xylem water potential versus hydraulic conductivity, suggested that the P50 value for Bigleaf Maple was -0.5 MPa; however, there was so little conductivity reduction after spinning several maple stems to this that I ended up spinning all Bigleaf Maple to -1.0 MPa. I spun all Coast Redwood stems to -6.0 MPa, close to the literature value for P50 of relatively short Coast Redwood trees.⁴⁶ After centrifugation, the Sperry apparatus was used to measure the minimum xylem hydraulic conductivity ($K_{h,min}$).

After measuring ($K_{h,min}$), the segments were recut underwater to ensure that the bark was flush with the xylem and that there were no obvious cracks in the bark near the cut ends. Only stems without side branches were chosen for the experimental sealed soaking treatment. Segments for sealed soaking treatment and negative controls were quickly patted dry on the ends and dipped in silicone sealant. The samples were then allowed to dry for approximately 1 hour (2 hours for Reed Bigleaf Maples). Positive controls (redwood only) had the ends temporarily wrapped in Parafilm during this time to reduce excess drying. After the sealant had hardened, negative controls were wrapped in Parafilm and placed in a sealed plastic bag on the benchtop; positive controls and sealed soaking treatment samples were placed in a deionized water bath and weighted down with a glass bowl to ensure all sides were in contact with water. All samples were left for 21 hours.

After 21 hours, sealant was removed, the sample ends recut several millimeters, and the final hydraulic conductivity measurements ($K_{h,post-treatment}$) taken using the Sperry apparatus. The stem, pith, and xylem diameter of each end of each segment was measured using calipers.

Benchtop Drydown Methods

Twelve Douglas-fir branches that included segments approximately 15 cm long and 0.8 cm in diameter were cut from marked trees using hand pruners. At least 5 cm was left between the cut end of the branch and the segment used for measurement. The branches were brought back to the laboratory, the cut ends wrapped in Parafilm, and placed on the laboratory floor with the lights on for approximately 58 hours to facilitate drying out of xylem tissue. The water potential of these branches was measured at four intervals during the drydown using a pressure chamber. The water potential of the branch tissues were allowed to equilibrate in a black plastic bag for at least two hours prior to each water potential measurement.⁴³ After the final water potential measurement, segments were excised underwater for hydraulic conductivity, prepared by removing bark near (~5 mm) the cut ends, wrapped in Parafilm to facilitate sealing, and $K_{h,min}$ measured using the Sperry apparatus.

After measurement of $K_{h,min}$, the ends of the segments were recut so that the xylem and bark were flush and the ends sealed with silicone sealant. Segments left on the benchtop for approximately one hour to allow the sealant to dry. Negative controls were then wrapped in Parafilm and placed in a sealed plastic bag; sealed soaking treatment samples placed in deionized water bath and weighted down with a glass bowl to ensure full contact with the water. Samples were left for 21 hours. After 21 hours, the sealant was removed, the samples recut underwater, the bark near the ends of the segments removed and the samples wrapped in Parafilm. $K_{h,post-treatment}$ was taken using the Sperry apparatus.

The segments were then vacuum infiltrated for 13 hours, the ends recut slightly, and $K_{h,max}$ measured using the Sperry apparatus. The stem, pith, and xylem diameter of each end of each segment was measured using calipers.

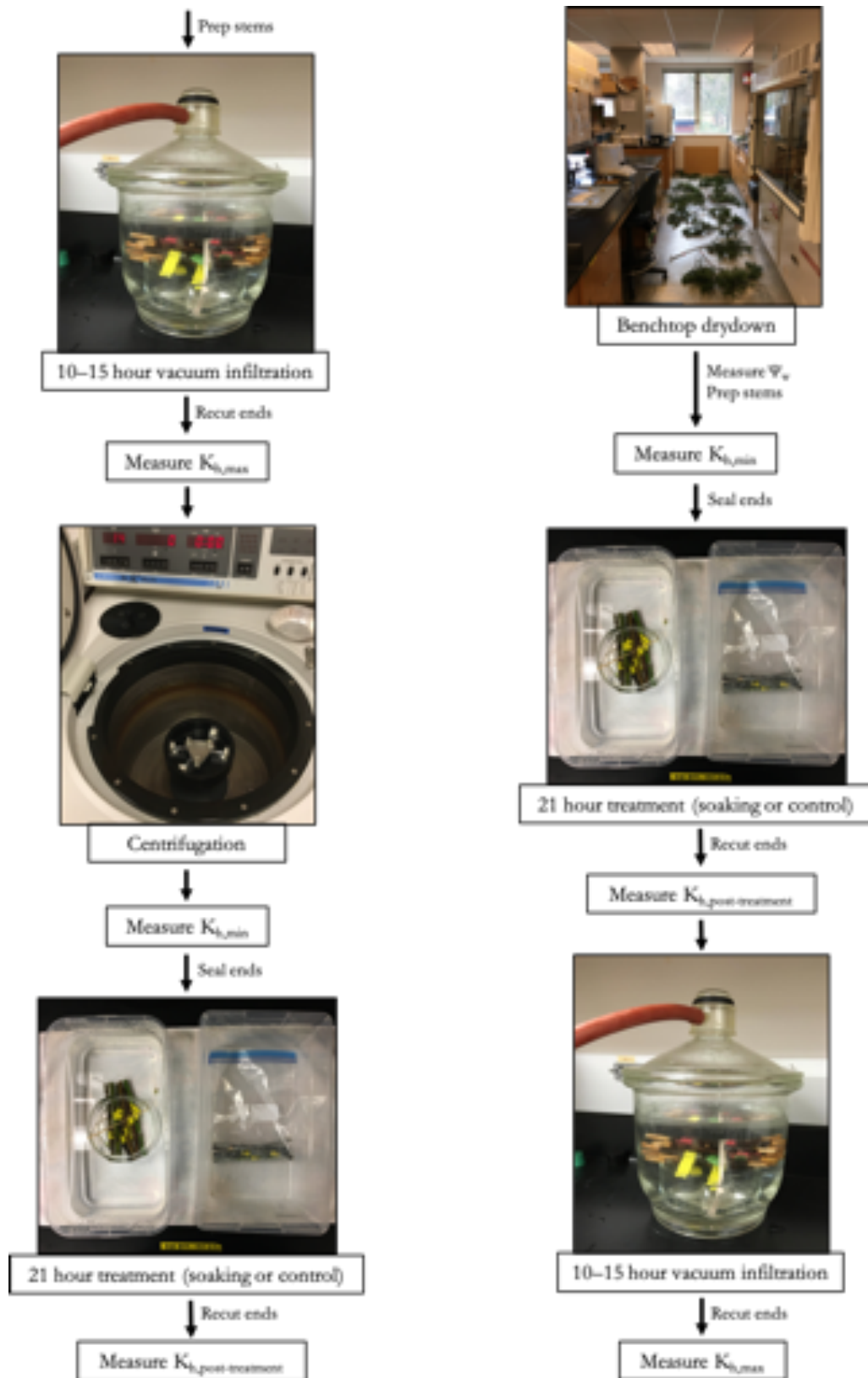


Figure 3.2. Flowcharts of centrifugation and drydown methods.

Calculations

Stem-specific hydraulic conductivity (K_s) values were calculated by dividing K_h by the mean xylem area of the segment. Percent loss in conductivity (PLC) was calculated for both K_{min} and $K_{post-treatment}$ values using the equation:

$$PLC = 100 * \left(1 - \frac{K_h}{K_{h,max}}\right) = 100 * \left(1 - \frac{K_s}{K_{s,max}}\right)$$

Once PLC was calculated, it was used to calculate “PLC difference.” This metric quantifies the relative decrease in embolism (increase in conductivity) for each branch after treatment:

$$PLC\ difference = PLC_{post-treatment} - PLC_{min}$$

Statistical Analyses

The means of relevant sample groups were compared using analyses of variance (ANOVAs) in R. The means of negative control groups were also compared to zero using one-sample T-tests in R. A *P*-value of less than 0.05 was considered significant (a 95 percent confidence interval). All boxplots were made using R. Asterisks or different letters indicate treatments that have values significantly different from one another.

Chapter 4: Results

Branch Age and Epiphyte Massing Results

Bigleaf Maple branch segments collected at the Sandy River site had significantly more epiphytes than did those collected at the Reed site. The mean dry mass of epiphytes was 0.0107 g on a Reed branch segment, versus 0.110 g on a Sandy branch segment (significant difference, $F_{1,22} = 7.4995$, $P = 0.01199$). However, the branches collected for sampling at Sandy were also significantly older than those collected at the Reed site, which could have contributed to the differences in epiphyte mass, as older branches have had longer to develop epiphytic communities. The mean branch age of the youngest part of the sampled segments was 11.1 years for Reed, 23.6 years for Sandy (significant difference, $F_{1,21} = 10.45$, $P = 0.00399$).

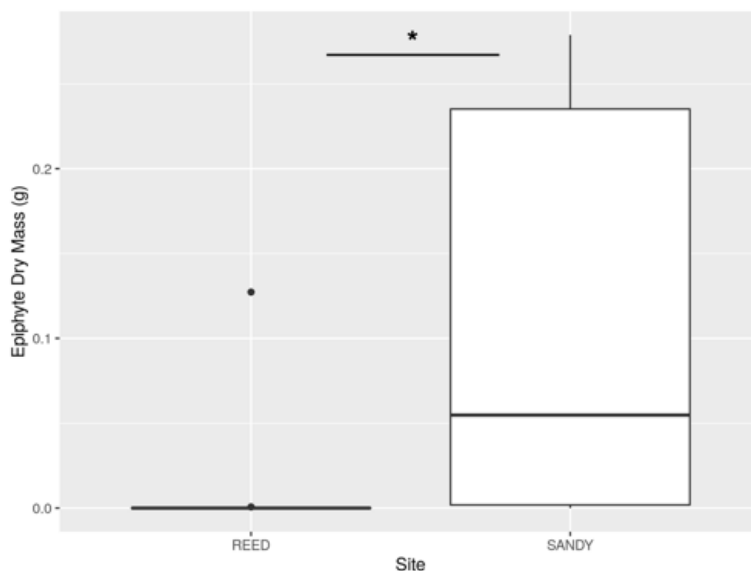


Figure 4.1. Epiphyte dry mass on Bigleaf Maple by site.

Boxplot of epiphyte dry mass on Bigleaf Maple branch segments used for hydraulic conductivity by site. The middle line on each boxplot indicates the median for the group; the bottom and top of the box indicate the first and third quartiles, respectively. Whiskers extend to include all points within 1.5 times the length of the box away from the ends of the box; dots are outliers outside of the whiskers range. Asterisk indicates treatments had means significantly ($P < 0.05$) different from one another. $n = 12$ for each site.

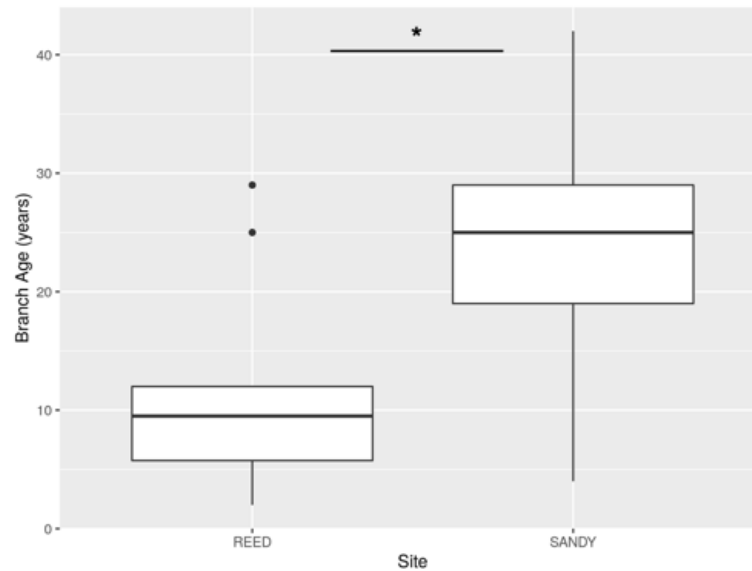


Figure 4.2. Branch age of Bigleaf Maple by site.

Boxplot of branch age of youngest part of branch segment used for hydraulic conductivity measurements by site. The middle line on each boxplot indicates the median for the group, while the bottom and top of the box indicate the first and third quartiles, respectively. Whiskers extend to include all points within 1.5 times the length of the box away from the ends of the box; dots are outliers outside of the whiskers range. Asterisk indicates treatments had means significantly different ($P < 0.05$) from one another. $n = 12$ for Reed, $n = 11$ for Sandy.

Dye Infiltration Test Results

Dye infiltration tests suggested that the efficacy of the sealant varied by species. Douglas-fir appeared to have successful sealing of 9 out of 10 branch segments, whereas Bigleaf Maple and Coast Redwood had less successful sealing: 7 out of 12 Coast Redwood branch ends and 8 out of 12 Bigleaf branch ends showed some evidence of leakage. However, even with the leakage, the positive controls showed much more staining than any of the sealed samples.

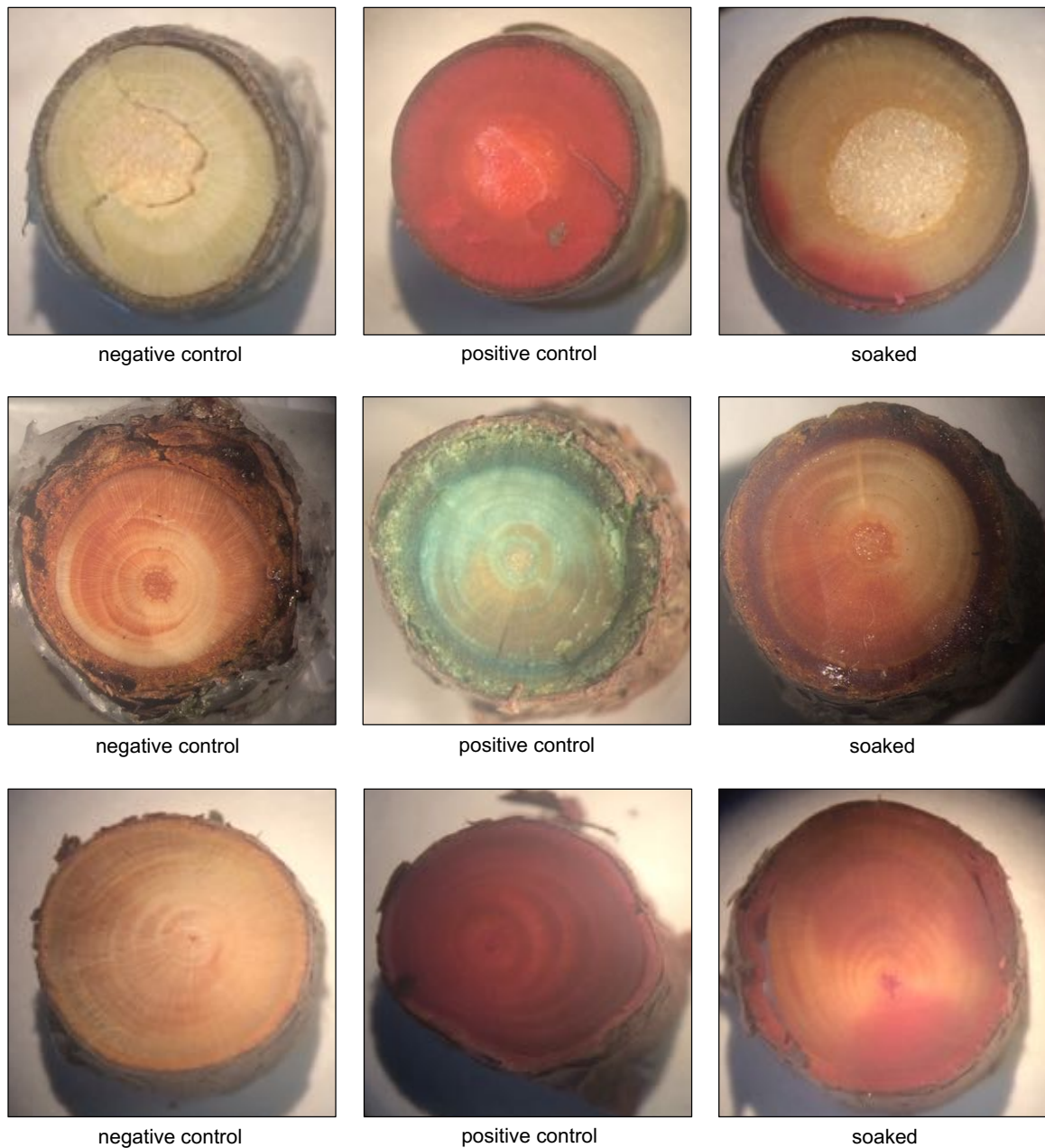


Figure 4.3. Dye infiltration test.

Bigleaf Maple (top), Douglas-fir (middle), and Coast Redwood (bottom). Negative controls were left on the benchtop for 24 hours; positive controls were soaked in the dye bath without sealant; soaked segments were sealed and placed in dye bath. Soaked segments that seemed roughly representative of leakage were imaged for this figure. Note that red dye was used for Bigleaf Maple and Coast Redwood, blue dye for Douglas-fir.

Evidence for Bark Water Uptake in Reed Bigleaf Maple

A comparison of absolute $K_{s,\text{post-treatment}}$ values of Reed Bigleaf Maple stems shows non-significant differences in conductivity between the control and soaked groups after the soaking treatment. Mean $K_{s,\text{max}}$ is $4.23 \text{ mg mm}^{-1} \text{ s}^{-1} \text{ kPa}$ for the negative control group and $4.02 \text{ mg mm}^{-1} \text{ s}^{-1} \text{ kPa}$ for the soaked group (no significant difference, $F_{1,9} = 0.1171$, $P = 0.74$); mean $K_{s,\text{min}}$ is $3.17 \text{ mg mm}^{-1} \text{ s}^{-1} \text{ kPa}$ for the negative control group and $2.91 \text{ mg mm}^{-1} \text{ s}^{-1} \text{ kPa}$ for the soaked group (no significant difference, $F_{1,9} = 0.427$, $P = 0.5298$); and mean $K_{s,\text{post-treatment}}$ is $3.19 \text{ mg mm}^{-1} \text{ s}^{-1} \text{ kPa}$ for the negative control group and $3.77 \text{ mg mm}^{-1} \text{ s}^{-1} \text{ kPa}$ for the soaked group (no significant difference, $F_{1,9} = 1.5861$, $P = 0.2396$).

When PLC is compared instead, the difference between control and soaked groups after treatment is significant. The mean PLC after centrifugation was 24.9 percent for the negative control group, 25.7 percent for the soaked group (no significant difference, $F_{1,9} = 0.0115$, $P = 0.9171$); after soaking treatment, the mean PLC for the control group was 25.0 percent compared with 4.77 percent for the soaked group (significant difference, $F_{1,9} = 16.238$, $P = 0.002974$).

The PLC difference is also significantly different between the treatment groups, with the soaked group decreasing substantially in PLC while the negative control group does not. The mean difference in PLC is +0.108 percent for the control compared with -20.9 percent for the soaked group (significant difference, $F_{1,9} = 14.014$, $P = 0.004601$). For the negative control group, this PLC difference is not significantly different from zero (one-sample T-test, $P = 0.9785$).

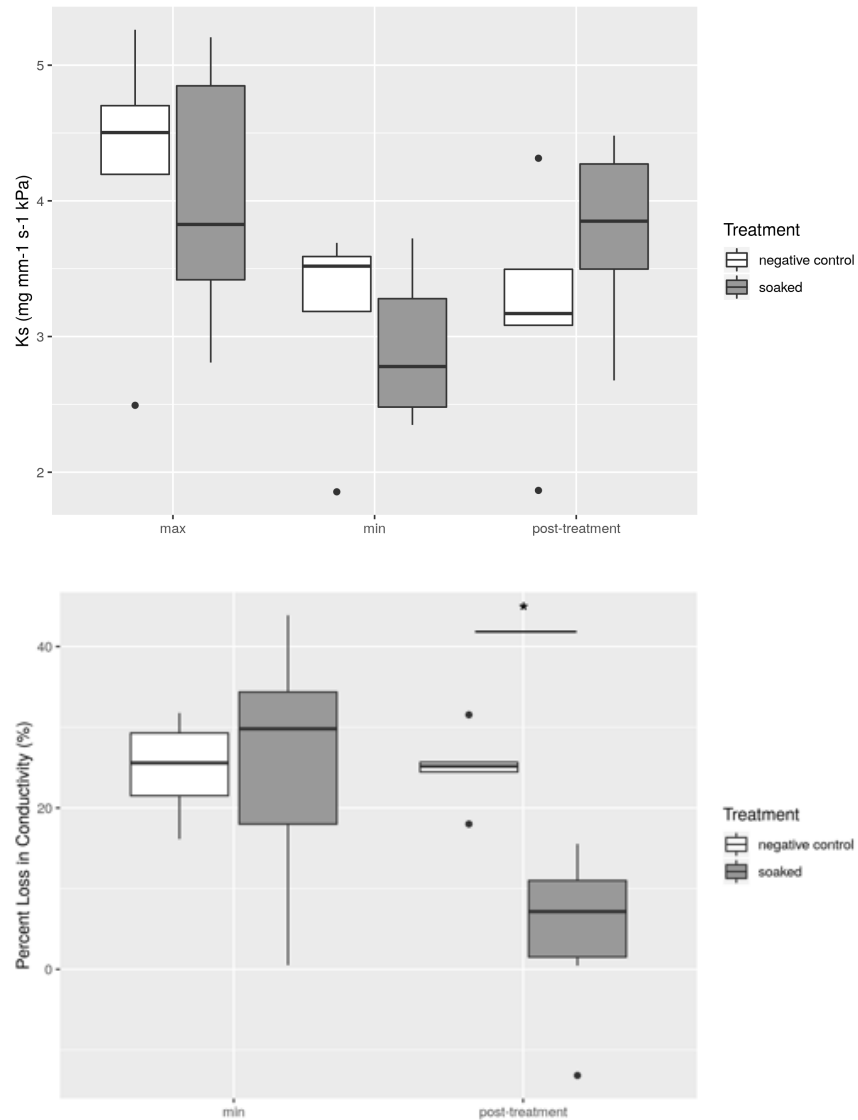


Figure 4.4. K_s and PLC of Reed Bigleaf Maple.

Boxplot of absolute and relative conductivity in Reed Bigleaf Maple. Stem-specific hydraulic conductivity (K_s) values (top) show absolute conductivity differences; PLC values (bottom) show relative differences in centrifuge-induced embolism and embolism recovery. The middle line on each boxplot indicates the median for the group, while the bottom and top of the box indicate the second and third quartiles, respectively. Whiskers extend up to 1.5 times the length of the box, and dots represent outliers. Asterisk indicates treatments that had means significantly different ($P < 0.05$) from one another. $n = 6$ for the soaked group, $n = 5$ for the negative control.

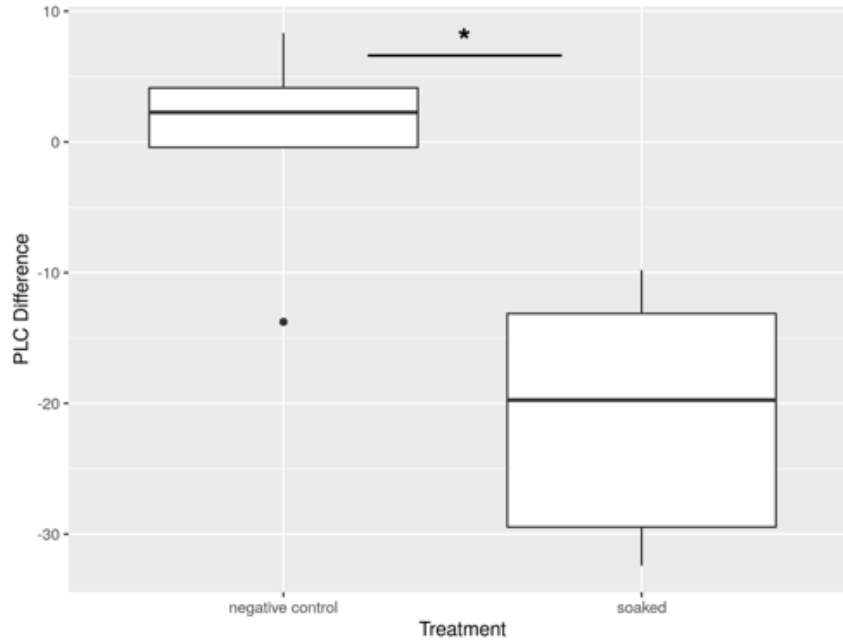


Figure 4.5. PLC difference in Reed Bigleaf Maple.

Boxplot of PLC difference for Bigleaf Maple at Reed site. The middle line on each boxplot indicates the median for the group, while the bottom and top of the box indicate the second and third quartiles, respectively. Whiskers extend up to 1.5 times the length of the box, and dots represent outliers. Asterisk indicates treatments had mean significantly different ($P < 0.05$) from one another. $n = 6$ for soaked group, $n = 5$ for negative control.

Evidence for Bark Water Uptake in Douglas-fir

Since it is impossible to dry different branches down to exactly the same water potential, it was expected that the $K_{s,min}$ and PLC_{min} would be more variable in Douglas-fir than in either Coast Redwood and Bigleaf Maple, which both induced embolism using centrifugation. Mean water potential of Douglas-fir after drydown and immediately prior to $K_{s,min}$ measurement was -3.62 MPa (standard deviation 0.598 MPa).

The mean $K_{s,max}$ was $0.266 \text{ mg mm}^{-1} \text{ s}^{-1} \text{ kPa}$ for the negative control, $0.288 \text{ mg mm}^{-1} \text{ s}^{-1} \text{ kPa}$ for soaked group (no significant difference, $F_{1,10} = 0.0525$, $P = 0.8233$); mean $K_{s,min}$ was $0.120 \text{ mg mm}^{-1} \text{ s}^{-1} \text{ kPa}$ for negative control, $0.122 \text{ mg mm}^{-1} \text{ s}^{-1} \text{ kPa}$ for soaked group (no significant difference, $F_{1,10} = 0.0139$, $P = 0.9086$); and mean $K_{s,post-treatment}$ was $0.127 \text{ mg mm}^{-1} \text{ s}^{-1} \text{ kPa}$ for negative control, $0.152 \text{ mg mm}^{-1} \text{ s}^{-1} \text{ kPa}$ for soaked group (no significant difference, $F_{1,10} = 0.1465$, $P = 0.7099$).

The mean percent loss in conductivity after drydown was substantially higher for the negative control group than for the soaked group, although not significantly so. The mean PLC after drydown was 59.5 percent for negative control, 72.0 percent for negative control (no significant difference, $F_{1,10} = 1.1882$, $P = 0.3013$). After treatment, the PLC was nearly the same for each treatment group. Mean PLC after treatment was 56.0 percent for the negative control group and 56.3 percent for the soaked stems (no significant difference, $F_{1,10} = 0.001$, $P = 0.975$)

There was a significant difference in the PLC difference between the negative control and soaked treatment groups. Mean PLC difference was -3.48 for negative control, -15.7 for soaked group (significant difference, $F_{1,10} = 11.481$, $P = 0.006905$). The mean PLC difference of the negative control was not significantly different from zero (one-sample T-test, $P = 0.1352$)

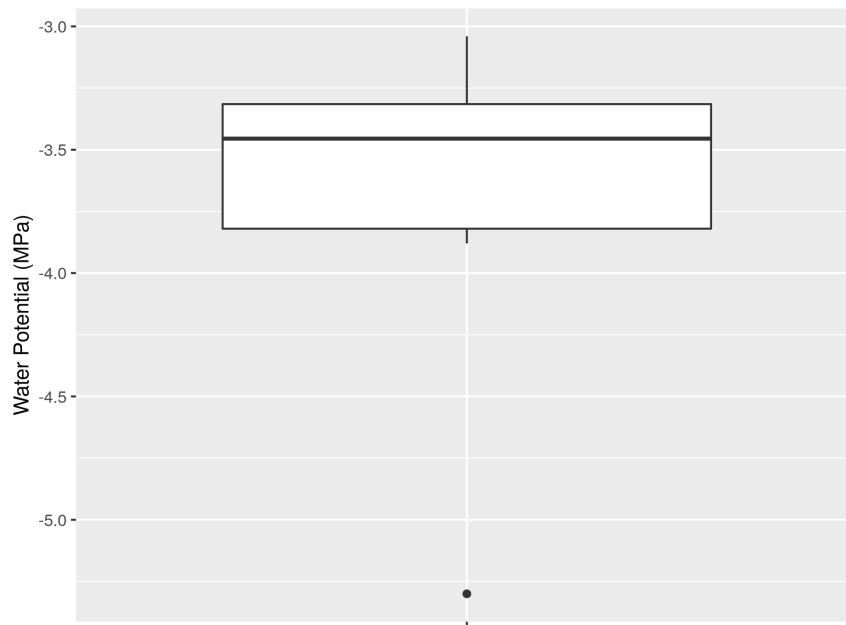


Figure 4.6. Douglas-fir water potential prior to $K_{s,min}$ measurement.

Boxplot of Douglas-fir water potential measured with pressure chamber prior to excision of branch segments for $K_{s,min}$ measurement, shown to visualize spread of pressure values. The middle line on the boxplot indicates the median value, while the bottom and top of the box indicate the second and third quartiles, respectively. Whiskers extend up to 1.5 times the length of the box, and the dot represents an outlier. $n = 12$.

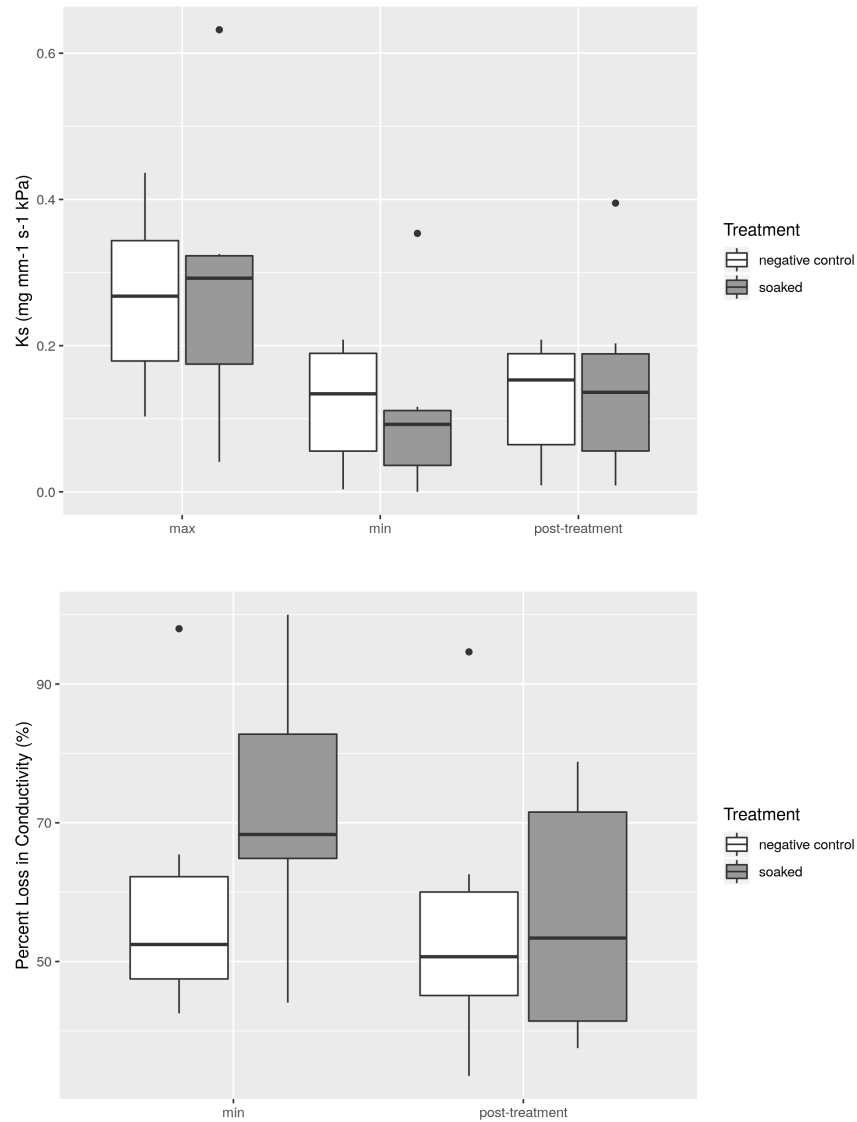


Figure 4.7. K_s and PLC of Douglas-fir.

Boxplot of absolute and relative conductivity in Reed Douglas-fir. Stem-specific hydraulic conductivity (K_s) values (top) show absolute conductivity; PLC values (bottom) show relative differences in centrifuge-induced embolism and embolism recovery. The middle line on each boxplot indicates the median for the group, while the bottom and top of the box indicate the second and third quartiles, respectively. Whiskers extend up to 1.5 times the length of the box, and dots represent outliers. No asterisk indicates that no treatments had means significantly different ($P < 0.05$) from one another $n = 6$ for each treatment group.

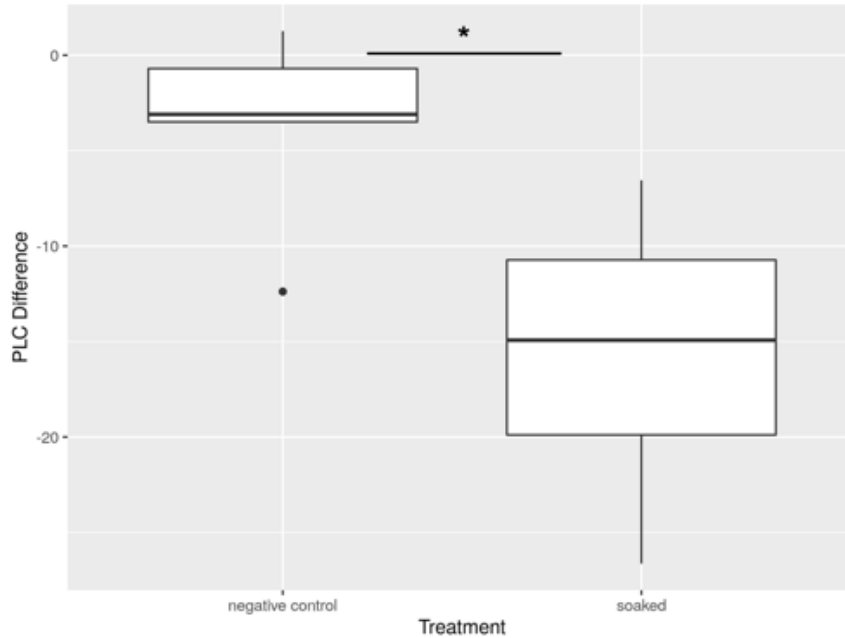


Figure 4.8. PLC difference in Douglas-fir.

Boxplot of PLC difference for Douglas-fir at Reed. The middle line on each boxplot indicates the median for the group, while the bottom and top of the box indicate the second and third quartiles, respectively. Whiskers extend up to 1.5 times the length of the box, and dots represent outliers. Asterisk indicates treatments had values significantly different ($P < 0.05$) from one another. $n = 6$ for each treatment group.

Evidence for Bark Water Uptake in Coast Redwood

Analysis of K_s values found no significant differences by treatment groups at any of the time points. Mean $K_{s,max}$ was $0.504 \text{ mg mm}^{-1} \text{ s}^{-1} \text{ kPa}$ for negative control, $0.530 \text{ mg mm}^{-1} \text{ s}^{-1} \text{ kPa}$ for positive control, $0.389 \text{ mg mm}^{-1} \text{ s}^{-1} \text{ kPa}$ for soaked group (no significant difference between soaked and negative control, $F_{1,10} = 0.4986$, $P = 0.4962$; no significant difference between soaked and positive control, $F_{1,10} = 0.7137$, $P = 0.418$; no significant difference between negative and positive controls, $F_{1,10} = 0.0178$, $P = 0.8965$). Mean $K_{s,min}$ was $0.128 \text{ mg mm}^{-1} \text{ s}^{-1} \text{ kPa}$ for negative control, $0.209 \text{ mg mm}^{-1} \text{ s}^{-1} \text{ kPa}$ for positive control, $0.153 \text{ mg mm}^{-1} \text{ s}^{-1} \text{ kPa}$ for soaked group (no significant difference between soaked and negative control, $F_{1,10} = 0.1863$, $P = 0.6751$; no significant difference between soaked and positive control, $F_{1,10} = 0.4264$, $P = 0.5285$; no significant difference between negative and positive controls, $F_{1,10} = 0.9892$, $P = 0.3434$). Mean $K_{s,post-treatment}$ was 0.297

mg mm⁻¹ s⁻¹ kPa for negative control, 0.489 mg mm⁻¹ s⁻¹ kPa for positive control, 0.377 mg mm⁻¹ s⁻¹ kPa for soaked group (no significant difference between soaked and negative control, $F_{1,10} = 0.4295$, $P = 0.527$; no significant difference between soaked and positive control, $F_{1,10} = 0.463$, $P = 0.5117$; no significant difference between positive and negative controls, $F_{1,10} = 1.5774$, $P = 0.2377$).

Mean PLC after centrifugation (PLC_{min}) was 72.7 percent for negative control, 64.4 percent for positive control, and 63.2 percent for soaked group (no significant difference between soaked and negative control, $F_{1,10} = 3.7014$, $P = 0.08327$; no significant difference between soaked and positive control, $F_{1,10} = 0.0504$, $P = 0.8268$; no significant difference between positive and negative controls, $F_{1,10} = 2.5437$, $P = 0.1418$). The mean PLC after treatment was significantly higher for the negative control group than for the soaked group, and slightly and non-significantly higher for the positive control group than for the soaked group. Mean PLC_{post-treatment} was 34.1 percent for negative control, 10.3 percent for positive control, and 5.95 for soaked group (significant difference between soaked and negative control, $F_{1,10} = 6.3517$, $P = 0.03037$; no significant difference between soaked and positive control, $F_{1,10} = 0.3594$, $P = 0.5622$; no significant difference between negative and positive controls, $F_{1,10} = 4.4535$, $P = 0.06101$).

Uniquely among the three species measured, even the negative control group showed substantial reduction in embolism following treatment. The mean PLC difference was -38.6 percent for the negative control, -54.2 percent for the positive control, and -57.3 percent for the soaked stems (significant difference between negative control and soaked, $F_{1,10} = 4.9679$, $P = 0.04994$; no significant difference between positive control and soaked, $F_{1,10} = 0.3229$, $P = 0.5824$; no significant difference between positive and negative controls, $F_{1,10} = 3.749$, $P = 0.08159$). The mean PLC difference of the negative control was significantly different from zero (one-sample T-test, $P = 0.003138$).

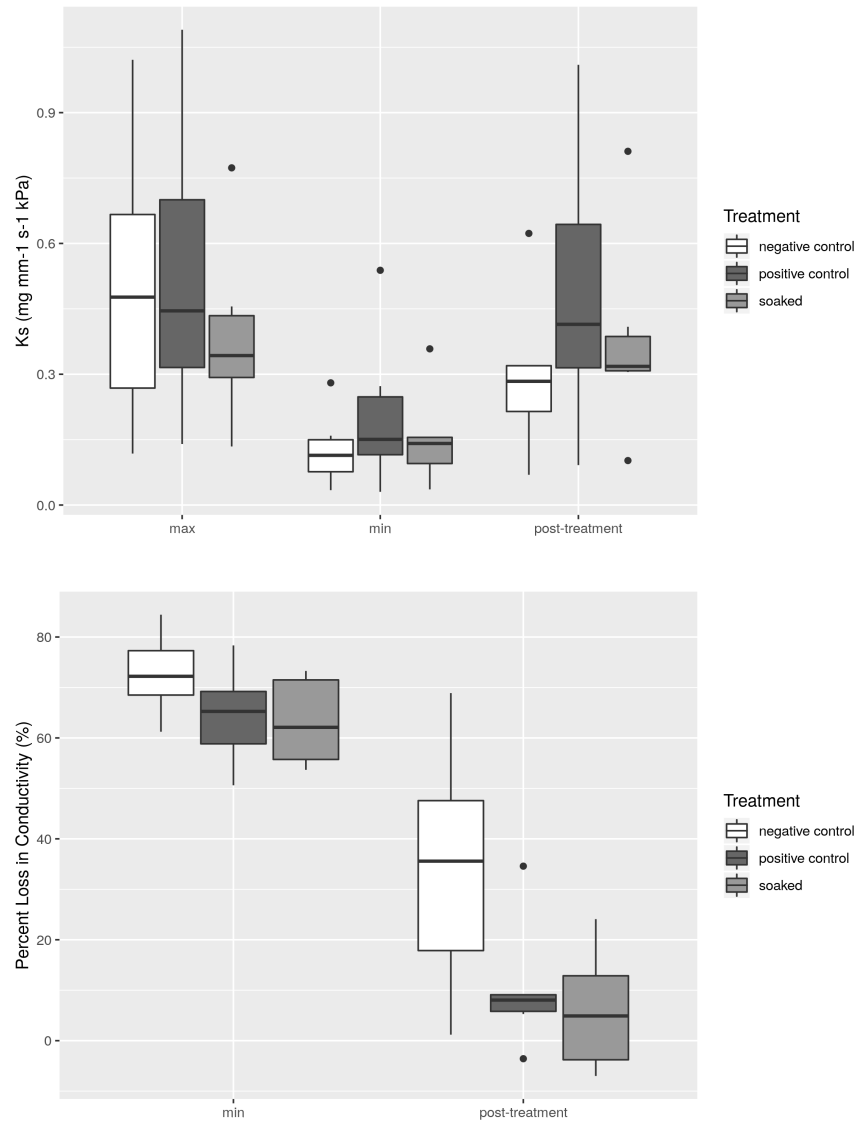


Figure 4.9. K_s and PLC of Coast Redwood.

Boxplot of absolute and relative conductivity in Reed Coast Redwood. Stem-specific hydraulic conductivity (K_s) values (top) show absolute conductivity; PLC values (bottom) show relative differences in centrifuge-induced embolism and embolism recovery. The middle line on each boxplot indicates the median for the group, while the bottom and top of the box indicate the second and third quartiles, respectively. Whiskers extend up to 1.5 times the length of the box, and dots represent outliers. Lack of asterisk indicates that no treatments had means significantly different ($P < 0.05$) from one another. $n = 6$ for each treatment group.

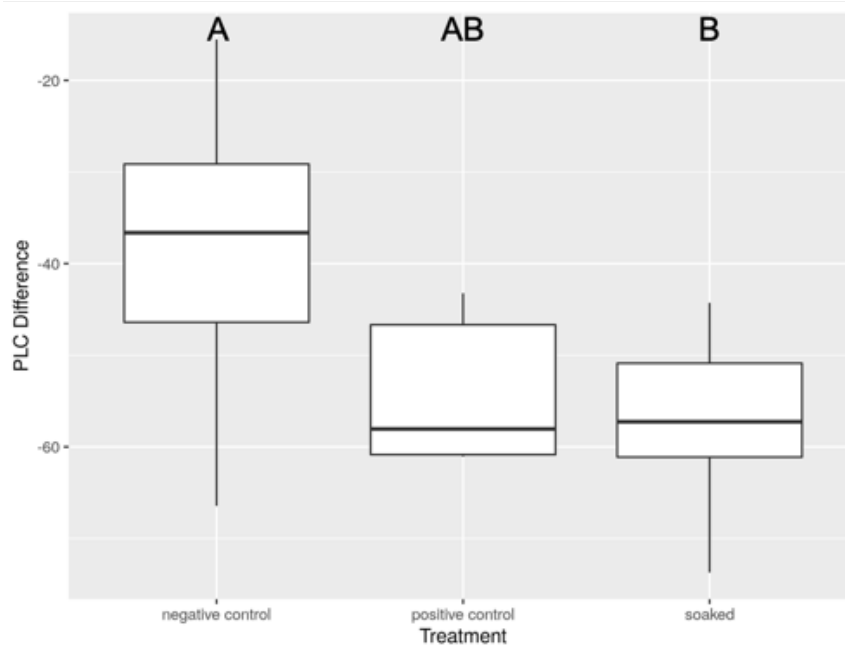


Figure 4.10. PLC difference in Coast Redwood.

Boxplot of PLC difference for Coast Redwood at Reed. The middle line on each boxplot indicates the median for the group, while the bottom and top of the box indicate the second and third quartiles, respectively. Whiskers extend up to 1.5 times the length of the box. Different letters correspond to treatments that have means significantly ($P < 0.05$) different from one another. $n = 6$ for each treatment group.

Conductivity Differences by Tree Species

Bigleaf Maple trees had significantly higher hydraulic conductivity at every stage than did either conifer species, with K_s values more than an order of magnitude greater than the K_s values for either conifer species. Mean $K_{s,max}$ values were $4.117 \text{ mg mm}^{-1} \text{ s}^{-1} \text{ kPa}$ for Bigleaf Maple, $0.474 \text{ mg mm}^{-1} \text{ s}^{-1} \text{ kPa}$ for Coast Redwood, and $0.277 \text{ mg mm}^{-1} \text{ s}^{-1} \text{ kPa}$ for Douglas-fir (all species have $K_{s,max}$ significantly different from one another, $P < 0.05$ for all pairwise comparisons). Mean $K_{s,min}$ values were $3.027 \text{ mg mm}^{-1} \text{ s}^{-1} \text{ kPa}$ for Bigleaf Maple, $0.116 \text{ mg mm}^{-1} \text{ s}^{-1} \text{ kPa}$ for Douglas-fir, and $0.163 \text{ mg mm}^{-1} \text{ s}^{-1} \text{ kPa}$ for Coast Redwood (significant difference between Bigleaf Maple and Douglas-fir $K_{s,min}$, $F_{1,21} = 246.76$, $P < 0.001$; significant difference between Bigleaf Maple and Coast Redwood $K_{s,min}$, $F_{1,27} = 351.3$, $P < 0.001$; no significant difference between Douglas-fir and Coast Redwood $K_{s,min}$, $F_{1,28} = 1.1384$, $P = 0.2951$). Differences between treatment

groups within species and $K_{s, \text{post-treatment}}$ values are discussed individually for each species earlier in this chapter.

Percent loss in conductivity also differed by species. Bigleaf Maple had the lowest PLC values after centrifugation (PLC_{\min}), while Douglas-fir and Coast Redwood had similar and much higher PLC values. Douglas-fir also had a greater range of PLC values, almost certainly due to the use of drydown instead of centrifugation for this species. Mean PLC_{\min} values were 25.29 percent for Bigleaf Maple, 65.73 percent for Douglas-fir, and 66.80 percent for Coast Redwood (significant difference between Bigleaf Maple and Douglas-fir PLC_{\min} , $F_{1,21} = 33.827$, $P < 0.001$; significant difference between Bigleaf Maple and Coast Redwood PLC_{\min} , $F_{1,27} = 109.37$, $P < 0.001$; no significant difference between Douglas-fir and Coast Redwood PLC_{\min} , $F_{1,28} = 0.0388$, $P = 0.8452$). Differences between treatment groups within species and $\text{PLC}_{\text{post-treatment}}$ values are discussed individually for each species earlier in this chapter.

PLC difference was most negative for Coast Redwood and least negative for Douglas-fir, with Bigleaf Maple PLC difference just slightly more negative than Douglas-fir. Coast Redwood is also the only species that has PLC difference of the negative control significantly different from zero by one-sample T-test. All three species have PLC differences of soaked group significantly different from negative control group. The lowest mean PLC difference for soaked samples is seen in Douglas-fir (soaked -15.65, negative control -3.48; significant difference, $F_{1,10} = 11.481$, $P = 0.006905$). Bigleaf Maple soaked samples have intermediate PLC difference (soaked -20.89, negative control +0.11; significant difference, $F_{1,9} = 14.014$, $P = 0.004601$). Coast Redwood have the highest PLC difference in all treatment groups (soaked -57.28, negative control -38.60, positive control -54.18; significant difference between negative control and soaked, $F_{1,10} = 4.9679$, $P = 0.04994$; no significant difference between positive control and soaked, $F_{1,10} = 0.3229$, $P = 0.5824$; no significant difference between positive and negative controls, $F_{1,10} = 3.749$, $P = 0.08159$).

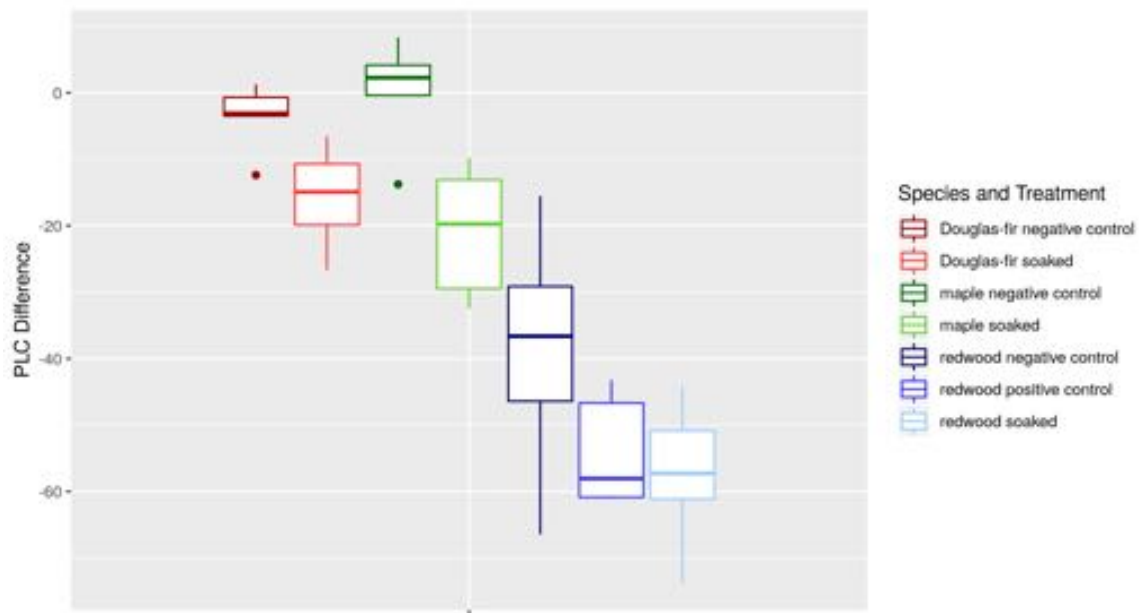


Figure 4.11. PLC difference in Reed trees by species and treatment.

Boxplot of PLC difference for Douglas-fir (reds), Bigleaf Maple (greens), and Coast Redwood (blues) by treatment. The middle line on each boxplot indicates the median for the group, while the bottom and top of the box indicate the second and third quartiles, respectively. Whiskers extend up to 1.5 times the length of the box, and dots represent outliers. $n = 6$ for each group except negative control Bigleaf Maple, where $n = 5$.

Chapter 5: Discussion

All three tree species tested showed some evidence of xylem embolism reduction in the soaking treatment stems compared with negative controls.

Epiphytes did not seem to improve bark water absorption in the only species where epiphytes were measured, Bigleaf Maple. In fact, although the Bigleaf Maple branch segments collected at the Sandy River site had significantly more epiphytes than did those collected at the Reed site, xylem embolism was reduced more post-soak with respect to negative controls in Reed segments than in Sandy segments; although there was a slight reduction in xylem embolism in soaked Sandy segments compared with controls, it was not significant (see Appendix B for Sandy Bigleaf Maple hydraulic data). The Sandy segments all had consistently lower K_s values than the Reed segments, suggesting that they were not necessarily comparable to the Reed segments. Because of this, I cannot definitively say that epiphytes have any effect on Bigleaf Maple bark permeability to water in isolated branch segments in a laboratory setting. Further, the methods used to study epiphyte effects do not take into account the potential importance of epiphytes as external water reservoirs on trees, since the prodigious water-holding capacity of epiphytes could keep bark moist for longer under field conditions. Additional work comparing the amount of time and magnitude of bark wetting in epiphyte-covered versus epiphyte-free branches is required.

Percent loss in conductivity differed by species, with Bigleaf Maple suffering much less embolism after centrifugation than either conifer species, which could have affected the ability of the segments to repair emboli — the larger the air embolism, the more water pressure is required to force the bubbles back into solution.⁴⁷ Bigleaf Maple was spun at -1.0 MPa after -0.5 MPa failed to induce significant embolism, despite being the measured P50 for Reed Bigleaf Maple trees in summer 2019.⁴⁸ This suggests that dormancy in Bigleaf Maple potentially decreases vulnerability to embolism. The significantly higher stem-specific hydraulic conductivity (K_s) values for Bigleaf Maple

than either conifer species were expected, as angiosperms tend to have greater rates of maximum hydraulic conductivity than conifers.⁶

The tree species measured differed in their respective abilities to perform embolism repair after the soaking treatment. Bigleaf Maple soaked stems exhibited, on average, a 20.9 percent decrease in PLC from minimum conductivity following soaking treatment, while Douglas-fir had a 15.7 percent decrease. The difference make sense given what is known about differences between angiosperms and conifers: angiosperms tend to have a greater capacity for embolism repair due to smaller hydraulic safety margins; they experience greater embolism under environmental conditions than conifers.⁴⁹ Coast Redwood had the highest decrease in PLC, at 54.2 percent for soaked samples, but because the negative control also decreased significantly after treatment, it is likely that this is an overestimate of the capacity of Coast Redwood to repair xylem embolism. Additionally, there was no significant difference between the PLC difference of the soaked group and the positive control group in Coast Redwood, which suggests that either the sealant was indeed ineffective or that the bark of Coast Redwood it permeable enough that the amount of water that makes it through the bark is not the limiting factor in embolism repair.

Dye infiltration test results revealed that the sealant procedure used was not sufficient to eliminate all water entry through cut surfaces, although the amount of dye entry into sealed segments was substantially less than in unsealed positive control stems. Therefore, the amount of bark water uptake may be overestimated in some cases, particularly in Coast Redwood and Bigleaf Maple, which saw greater leakage than Douglas-fir. Further development of the Mason Earles (2016) method used to test for branch water uptake is required.

Chapter 6: A Broader Context

As climate change causes the seasonality of the Mediterranean-type climate of the Pacific Northwest to become more extreme, the region will experience longer dry periods, more frequent droughts, and hotter temperatures. These conditions will combine into a “perfect storm” of increased transpiration and decreased available water, causing plants to experience increased xylem cavitation, and therefore decreased ability to transport water, particularly in very tall trees, which already face difficulties transporting water from their roots to their crowns. Whether the forests of the Pacific Northwest will survive as we know them today will depend on the ability of tree species to adapt to these new conditions.

If later work confirms my results, some amount of embolism reduction is possible through bark water absorption in these trees. The PLC difference of soaked segments in this lab-based experiment represents an upper bound for embolism reversal due to bark water uptake for each species. The isolated branch segments that I used did not have the negative pressure gradient of xylem tissue acting on them — in fact, because the segments were held underwater, there was likely some positive pressure acting on them, which may have aided in embolism dissolution. However, it is possible that canopy wetting events could reduce the xylem pressure gradient enough to dissolve emboli and increase xylem hydraulic conductivity in natural conditions as well. Additional work in a field setting is needed to evaluate the feasibility of this as a potential mechanism for reducing hydraulic stress in nature. Although natural conditions would likely result in much less bark water uptake than laboratory conditions, any embolism reduction is helpful to trees on the edge of hydraulic failure.

If bark water transport is common in nature, as my results suggest, it is unclear if climate change will prove to be more or less harmful for forests than predicted. On one hand, long periods of summer drought with no fog or damp air could prove even more detrimental for tree species that rely on canopy wetting to maintain hydraulic function. However, in trees that will receive less rainfall in the future but still be exposed to

summer fog, or have water-holding epiphyte masses that keep bark damp in dry conditions, bark water uptake — as a part of a canopy water absorption system that also includes foliar water uptake — could reduce some of the damage caused by hotter drought conditions.¹⁹

Appendix A: Glossary of Terms

Air seeding	The process of air emboli filling adjacent cells due to highly negative xylem pressures that pull air through the tiny pit membranes.
Angiosperm	Plants that produce flowers. Angiosperms include many tree species as well, including maples.
ANOVA	Analysis of variance. A statistical test used in this thesis to compare the means of different treatment groups to determine if differences between groups are statistically significant.
Anthropogenic	Human-caused
Cavitation	The process of embolism formation, when an air bubble expands under negative pressure in the xylem to fill an entire vessel element or tracheid.
Centrifugation	The process of spinning a sample in a centrifuge; used in this thesis to induce a specific negative pressure in the spun stem segment, which theoretically corresponds to a specific amount of embolism in the segment. ⁴³
Conifer	The most common and widespread group of the gymnosperms, the plants with “naked seeds,” seeds unprotected by an ovary or fruit. Conifers are characterized by needles or scaly leaves, and many produce cones.
Drydown	The process of allowing sample branches to dry out on a benchtop; used in this thesis to induce embolism. ⁴³
Embolism	The air bubbles present in xylem tissues due to cavitation. More negative xylem pressures mean more embolized tissue; more embolized tissue means lower hydraulic conductivity relative to the maximum (greater PLC)
Embolism repair	The process whereby embolism can be reversed. Known to occur when xylem pressures become positive enough to force some air bubbles back into solution; whether repair of embolism under the negative pressures found in most tree xylem is possible is not agreed upon. ⁴¹

Epiphyte	A plant or lichen that grows on other plants for the purpose of physical support. Common types of epiphytes in the Pacific Northwest are mosses, club mosses, lichens, and some fern species.
Gas exchange	The process of carbon dioxide entering plant leaves, and water and oxygen leaving, during photosynthesis. Gas exchange is necessary in order for plants to turn carbon dioxide into sugars, but it also results in very high water loss during photosynthetic activity.
Hydraulic conductivity (K_h or K_s)	A measurement of the flow-through rate of water through the xylem. K_h gives the hydraulic conductivity of the stem in units of $\text{mg mm s}^{-1} \text{ kPa}$, which takes into account the length but not the cross-sectional area of the stem. K_h can be divided by the cross-sectional area of the stem segment to get K_s , the stem-specific hydraulic conductivity (units of $\text{mg mm}^{-1} \text{ s}^{-1} \text{ kPa}$).
Maximum hydraulic conductivity ($K_{s,\text{max}}$ or $K_{h,\text{max}}$)	The hydraulic conductivity when no xylem embolism is present; the highest possible hydraulic conductivity for a specific branch segment. Found by measuring hydraulic conductivity after removing all emboli from branch segments through vacuum infiltration.
Mediterranean climate	Found on the western edges of major continents at mid-latitudes, a Mediterranean climate pattern is characterized by cool, mild, wet winters and hot, dry summers. The Pacific Northwest follows a Mediterranean-type rainfall pattern, with the majority of the precipitation falling as winter rain, but is too far north to be generally considered a true Mediterranean climate. ^{4,5}
Pacific Northwest	The coastal region of the northwestern United States and Canada that stretches from the northern California coast up to southwestern Alaska on the west side of the Cascade mountains. This area is characterized by cool, extremely wet winters and warm, relatively dry summers.
Percent loss in conductivity (PLC)	A measure of the relative effects on hydraulic conductivity of embolism present in xylem, compared to the maximum hydraulic conductivity. Calculated using the equation $\text{PLC} = 100 * \left(1 - \frac{K_h}{K_{h,\text{max}}}\right) = 100 * \left(1 - \frac{K_s}{K_{s,\text{max}}}\right)$

Perfusion solution	The solution of 20 mM potassium chloride (KCl) used for measuring hydraulic conductivity in a Sperry apparatus. Prevents the decreases in conductivity over time that occur if pure water is used for perfusion. ⁴²
Pits	Microscopic holes in the secondary wall of xylem cells, but particularly important in tracheids, which do not have the perforated end plates of vessel elements. Pit pairs (pits opposite to one another in adjacent cells) allow water movement between adjacent cells with minimal resistance. ⁷
PLC difference	A metric used in this thesis to quantify xylem embolism repair in samples before and after treatment. Calculated using the equation: $PLC\ difference = PLC_{post-treatment} - PLC_{min}$
Pressure chamber	A piece of equipment used for measuring water potential, a pressure chamber uses a tank of pressurized nitrogen gas to pressurize a small chamber with a twig placed in, cut end up. Nitrogen gas is allowed to flow slowly into the chamber as the cut end is observed with a magnifying glass. The negative pressure that the leaves create on the xylem water column is reduced as the pressure builds in the chamber on the leaf side of the twig. The positive pressure it takes to equalize the xylem pressure (observable when water begins flowing out of the cut end) can be recorded the water potential of the xylem.
Sperry apparatus	A piece of equipment used for measuring hydraulic conductivity, a Sperry apparatus consists of an IV bag containing perfusion solution, tubing, and a balance. A stem is connected to tubing at both ends such that perfusion solution can flow from the IV bag through the tubing and stem and into a collection container on the balance. An Excel program on a computer connected to the balance measures the mass of the solution flowing through the stem at regular intervals to calculate the flow-through rate of the stem; this rate, combined with the solution temperature, relative height of the IV bag, and stem length are used to calculate K_h .

Statistical significance	A threshold that quantifies the likelihood that a similarity or difference between treatment groups is due to random chance. In this thesis, statistical significant means a <i>P</i> -value less than 0.05.
Stomata	The pores on the leaves of plants through which gas exchange occurs. Stomata can close or open based on the favorability of the conditions; when they close to reduce water loss in hot, dry conditions, photosynthetic carbon assimilation is also reduced.
Tracheid	The long, narrow water conducting cells found in the xylem of all vascular plants. Pit pairs allow water movement between adjacent tracheids with minimal resistance. Conifers have a specialized “valve” to control water movement between pit pairs and reduce embolism movement. ⁷
Transpiration	The process of water moving through the vascular tissue of a plant and then evaporating through the leaves. Most water is lost during photosynthesis because of the necessity of keeping stomata open in order for gas exchange to occur.
Vacuum infiltration	The process of putting stem segments used for hydraulic conductivity measurements underwater in a sealed chamber and then placing the chamber under vacuum for a period of time (usually overnight, between 8 and 16 hours). The vacuum pulls all emboli out of the xylem vessels and fills them entirely with water. After vacuum infiltration, $K_{h,max}$ can be measured on the stems.
Vessel element	Vessel elements are another type of water-conducting xylem cell. They are shorter and wider than tracheids, and have perforated end plates that conduct water easily, allowing them to be stacked to form long vessels. They can conduct water at greater rates, but are also generally more susceptible to embolism. Conifers do not have vessel elements. ⁷
Vulnerability curve	A method for determining the relative susceptibility of a plant to embolism. It involves measuring the hydraulic conductivities at a set of known water potentials (through either drydown or centrifugation) and then graphing the

PLC by the water potential. The shape of a vulnerability curve varies widely by species.

Water potential (Ψ_w)

A measure of the negative pressure created in the xylem by transpiration off the leaf surfaces. Water potential is most commonly measured using a pressure chamber.

Xylem

The water conducting tissue of a vascular plant. Xylem is composed of non-living cells whose purpose is to conduct water and prevent embolism from forming and spreading. In conifers, tracheids are the only type of xylem cells, but in angiosperms, both tracheids and vessel elements make up the xylem.

Appendix B: Supplemental Information

Non-Significant Increases in Conductivity Following Soaking Treatment in Sandy Bigleaf Maple

A comparison of absolute K_s values of Bigleaf Maple stems shows non-significant differences in conductivity between the control and soaked groups after the soaking treatment. Mean $K_{s,max}$ is $2.31 \text{ mg mm}^{-1} \text{ s}^{-1} \text{ kPa}$ for negative control, $2.53 \text{ mg mm}^{-1} \text{ s}^{-1} \text{ kPa}$ for soaked (no significant difference, $F_{1,9} = 0.0917$, $P = 0.7689$); mean $K_{s,min}$ is $1.82 \text{ mg mm}^{-1} \text{ s}^{-1} \text{ kPa}$ for negative control, $1.95 \text{ mg mm}^{-1} \text{ s}^{-1} \text{ kPa}$ for soaked (no significant difference, $F_{1,9} = 0.0285$, $P = 0.8696$); mean $K_{s,post-treatment}$ is $1.65 \text{ mg mm}^{-1} \text{ s}^{-1} \text{ kPa}$ for negative control, $2.17 \text{ mg mm}^{-1} \text{ s}^{-1} \text{ kPa}$ for soaked (no significant difference, $F_{1,9} = 0.6207$, $P = 0.451$).

Comparison of PLC suggests that the PLC decreases more after treatment for the soaked stems than for the negative control stems, but this difference is not significant to the 95 percent confidence level. Mean PLC after centrifugation is 26.4 percent for negative control, 24.1 for soaked (no significant difference, $F_{1,9} = 0.0266$, $P = 0.874$); mean PLC after treatment was 30.3 percent for negative control, 14.1 percent for soaked (no significant difference, $F_{1,9} = 2.5398$, $P = 0.1455$).

A comparison of PLC difference also does not show a significant difference by treatment group, although the mean PLC difference is lower for the soaked group than it is for the negative control group. Mean PLC difference was +3.93 for negative control, -10.0 for soaked (no significant difference, $F_{1,9} = 1.2815$, $P = 0.2869$). The PLC difference of the negative control is not significantly different from zero (one-sample T-test, $P = 0.7201$), nor is the PLC difference of the soaked group (one-sample T-test, $P = 0.1191$).

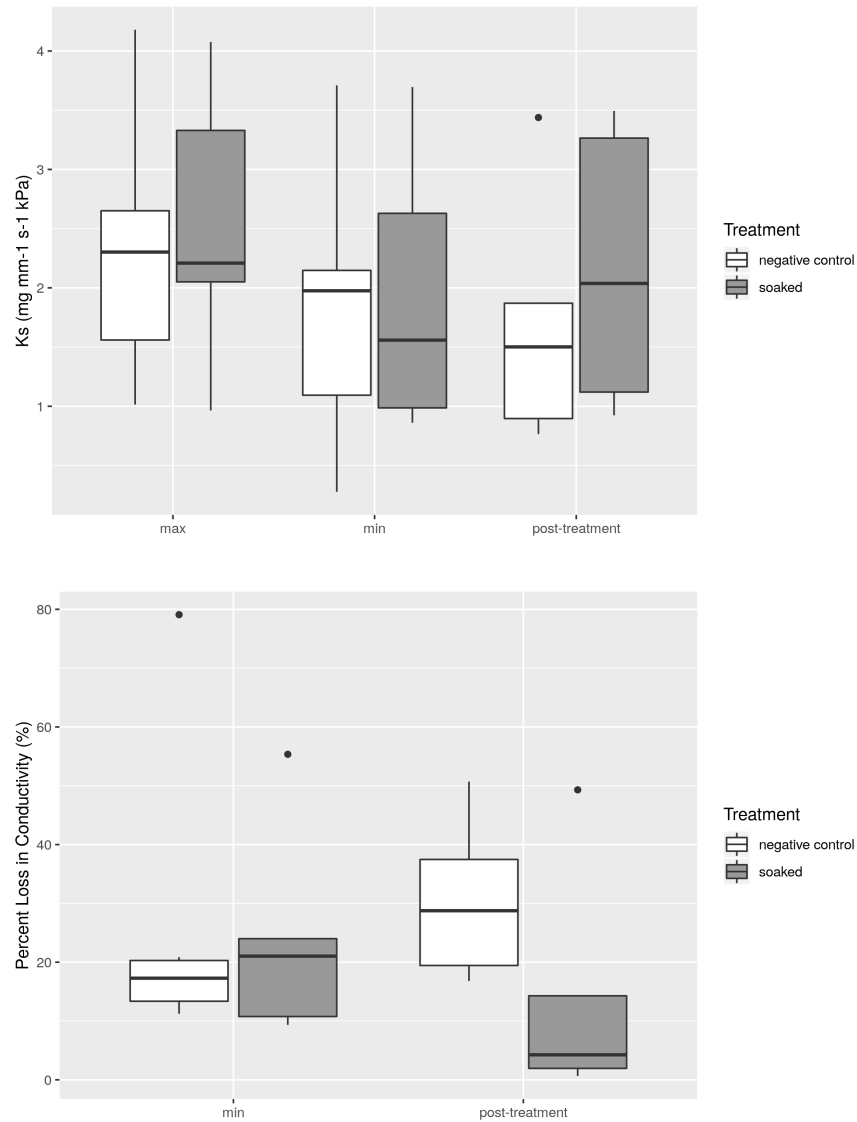


Figure B.1. K_s and PLC of Sandy Bigleaf Maple.

Boxplot of absolute and relative conductivity in Sandy Bigleaf Maple. Stem-specific hydraulic conductivity (K_s) values (top) show absolute conductivity; PLC values (bottom) show relative differences in centrifuge-induced embolism and embolism recovery. The middle line on each boxplot indicates the median for the group, while the bottom and top of the box indicate the second and third quartiles, respectively. Whiskers extend up to 1.5 times the length of the box, and dots represent outliers. Lack of asterisks indicates that there are no measurements where treatment groups have significantly different ($P < 0.05$) means. $n = 5$ for soaked group, $n = 6$ for negative control.

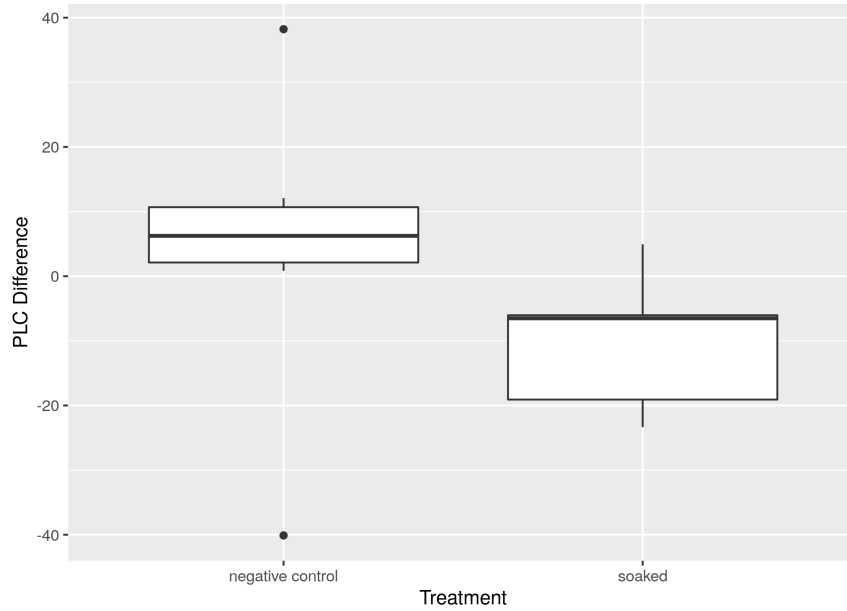


Figure B.2. PLC difference in Sandy Bigleaf Maple.

Boxplot of PLC difference for Bigleaf Maple at Sandy site. The middle line on each boxplot indicates the median for the group, while the bottom and top of the box indicate the second and third quartiles, respectively. Whiskers extend up to 1.5 times the length of the box, and dots represent outliers. $n = 5$ for the soaked group, $n = 6$ for the negative control.

Conductivity Differences in Reed and Sandy Bigleaf Maples

Bigleaf Maple samples collected from the Reed site had significantly higher hydraulic conductivity values than did those collected from the Sandy site. Mean $K_{s,max}$ for Reed Bigleaf Maple was $4.12 \text{ mg mm}^{-1} \text{ s}^{-1} \text{ kPa}$, compared with $2.41 \text{ mg mm}^{-1} \text{ s}^{-1} \text{ kPa}$ for Sandy (significant difference, $F_{1,20} = 14.94$, $P < 0.001$), and mean $K_{s,min}$ was $3.03 \text{ mg mm}^{-1} \text{ s}^{-1} \text{ kPa}$ for Reed, compared to $1.88 \text{ mg mm}^{-1} \text{ s}^{-1} \text{ kPa}$ for Sandy (significant difference, $F_{1,20} = 8.5358$, $P = 0.008437$). However, there was essentially no difference in centrifuge-induced PLC between the two sites, as the mean was 25.3 percent for both sites ($F_{1,20} = 0.011$, $P = 0.9953$) (see Figure 4.4 and Figure B.1). $K_{s,post-treatment}$ values are compared individually for each site.

PLC difference was not significantly different by site. Mean PLC difference was +0.108 for Reed negative control, -20.9 for Reed soaked treatment, +3.92 for Sandy negative control, and -10.0 for Sandy soaked treatment (PLC difference in negative control stems not significantly different by site, $F_{1,9} = 0.1023$, $P = 0.7564$; PLC difference in soaked stems not significantly different by site, $F_{1,9} = 2.8991$, $P = 0.1228$).

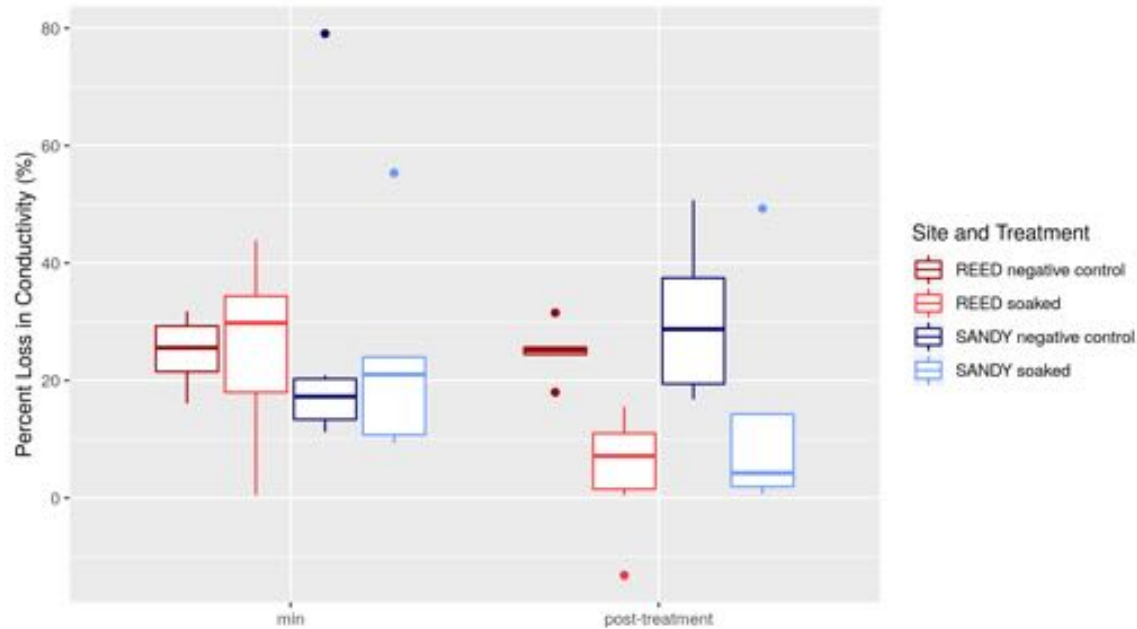


Figure B.3. K_s differences in Bigleaf Maple by site and treatment.

Boxplot of stem-specific hydraulic conductivity of Bigleaf Maple at Reed site (reds) and Sandy River site (blues). The middle line on each boxplot indicates the median for the group, while the bottom and top of the box indicate the second and third quartiles, respectively. Whiskers extend up to 1.5 times the length of the box, and dots represent outliers. $n = 6$ for Reed soaking treatment, $n = 5$ for Reed negative control, $n = 5$ for Sandy soaking treatment, $n = 6$ for Sandy negative control.

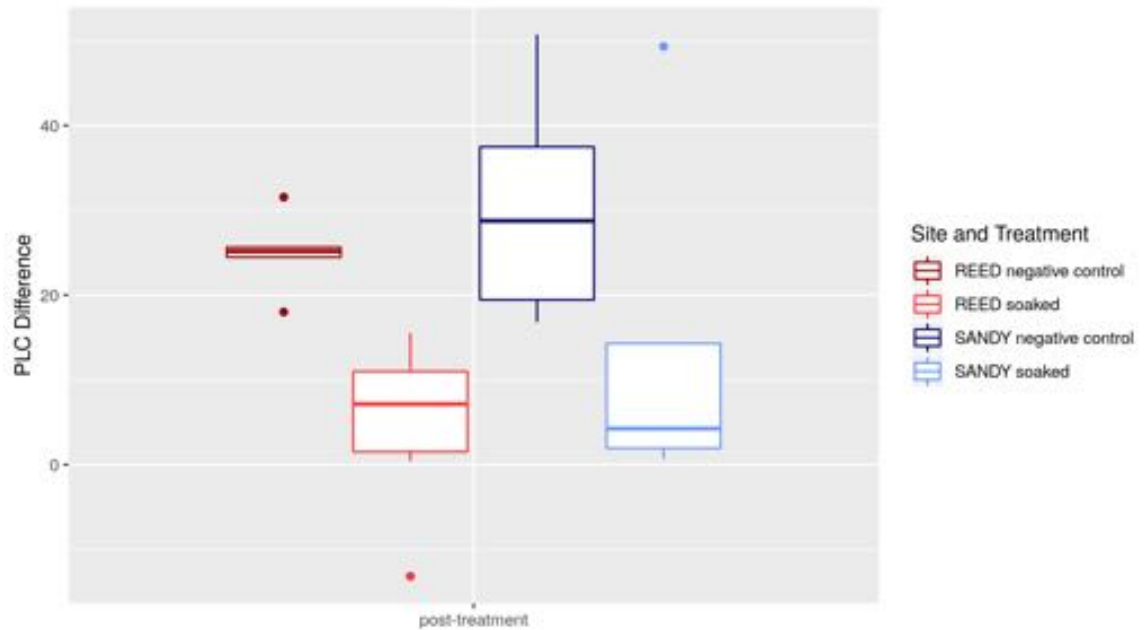


Figure B.4. PLC difference in Bigleaf Maple by site and treatment.

Boxplot of PLC difference for Bigleaf Maple at Reed site (reds) and Sandy River site (blues). The middle line on each boxplot indicates the median for the group, while the bottom and top of the box indicate the second and third quartiles, respectively. Whiskers extend up to 1.5 times the length of the box, and dots represent outliers. $n = 6$ for Reed soaking treatment, $n = 5$ for Reed negative control, $n = 5$ for Sandy soaking treatment, $n = 6$ for Sandy negative control.

References

1. Waring, R. H. & Franklin, J. F. Evergreen Coniferous Forests of the Pacific Northwest. *Science* **204**, 1380–1386 (1979).
2. Hammer, G. R. Climate of Oregon. 7.
3. The Editors of Encyclopaedia Britannica. Mediterranean Climate. *Encyclopedia Britannica* <https://www.britannica.com/science/Mediterranean-climate>.
4. Esler, K. J., Jacobsen, A. L. & Pratt, R. B. *The Biology of Mediterranean-Type Ecosystems*. (Oxford University Press, 2018).
doi:10.1093/oso/9780198739135.001.0001.
5. George, M. R. Mediterranean Climate.
http://rangelandarchive.ucdavis.edu/Annual_Rangeland_Handbook/Mediterranean_Climate.
6. Carnicer, J., Barbeta, A., Sperlich, D., Coll, M. & Peñuelas, J. Contrasting trait syndromes in angiosperms and conifers are associated with different responses of tree growth to temperature on a large scale. *Front. Plant Sci.* **4**, (2013).
7. Taiz, L. & Zieger, E. *Plant Physiology*. (Sinauer Associates, Inc., 2010).
8. Limm, E. B., Simonin, K. A., Bothman, A. G. & Dawson, T. E. Foliar water uptake: a common water acquisition strategy for plants of the redwood forest. *Oecologia* **161**, 449–459 (2009).
9. Gray, A. N., Monleon, V. J. & Spies, T. A. *Characteristics of remnant old-growth forests in the northern Coast Range of Oregon and comparison to surrounding landscapes*. PNW-GTR-790 <https://www.fs.usda.gov/treearch/pubs/33090> (2009)
doi:10.2737/PNW-GTR-790.
10. US Forest Service. California Coastal Steppe, Mixed Forest, and Redwood Forest Province. <https://www.fs.fed.us/land/ecosysmgmt/colorimagemap/images/263.html>.
11. Climate of Washington. <https://wrcc.dri.edu/narratives/WASHINGTON.htm>.
12. Nadkarni, N. M. Biomass and mineral capital of epiphytes in an *Acer macrophyllum* community of a temperate moist coniferous forest, Olympic Peninsula, Washington State. *Can. J. Bot.* **62**, 2223–2228 (1984).
13. Oak Woodlands – Oregon Conservation Strategy.
<https://oregonconservationstrategy.org/strategy-habitat/oak-woodlands/>.
14. Sherrod, D. Cascade Mountain Range in Oregon.
https://oregonencyclopedia.org/articles/cascade_mountain_range/.
15. US Forest Service. Cascade Mixed Forest — Coniferous Forest — Alpine Meadow Province.
<https://www.fs.fed.us/land/ecosysmgmt/colorimagemap/images/m242.html>.

16. Niemiec, S. S., Ahrens, G. R., Willits, S. & Hibbs, D. E. *Hardwoods of the Pacific Northwest*. (Forest Research Laboratory, 1995).
17. Eastern Cascades forests | Ecoregions | WWF. *World Wildlife Fund*
<https://www.worldwildlife.org/ecoregions/na0512>.
18. City, M. A. 1111 S. S. C. & Us, C. 95531 P.-6101 C. Economic Impacts of National Park Visitation Increase - Redwood National and State Parks (U.S. National Park Service). <https://www.nps.gov/redw/learn/news/econ.htm>.
19. Mason Earles, J. *et al.* Bark water uptake promotes localized hydraulic recovery in coastal redwood crown: Localized hydraulic recovery via bark water uptake. *Plant Cell Environ.* **39**, 320–328 (2016).
20. US Forest Service. *Pseudotsuga menziesii* var. *menziesii*.
<https://www.fs.fed.us/database/feis/plants/tree/psemenm/all.html>.
21. Lavender, D. P. & Richard K. Hermann. *Douglas-fir: The Genus Pseudotsuga*. (Oregon Forest Research Laboratory, 2014).
22. This Tree Might Reach to China. *The Morning Times* (1897).
23. Franklin, J. F. *et al.* *Ecological Characteristics of Old-Growth Douglas-fir Forests*. (1981).
24. Fryer, J. L. *Acer macrophyllum*, Bigleaf Maple. *Fire Effects Information System*
<https://www.fs.fed.us/database/feis/plants/tree/acemac/all.html> (2011).
25. Kenkel, N. C. & Bradfield, G. E. Epiphytic vegetation on *Acer macrophyllum*: a multivariate study of species-habitat relationships. 11 (1986).
26. Hargis, H. *et al.* Arboreal Epiphytes in the Soil-Atmosphere Interface: How Often Are the Biggest “Buckets” in the Canopy Empty? *Geosciences* **9**, 342 (2019).
27. The Editors of Encyclopaedia Britannica. Moss. *Encyclopedia Britannica*
<https://www.britannica.com/plant/moss-plant>.
28. Pugnaire, F. I. & Valladares, F. *Functional Plant Ecology*. (CRC Press, 2007).
29. Krosnick, S. & Indoe, K. E. What is a bryophyte anyway? *The New York Botanical Garden* <https://sciweb.nybg.org/science2/hcol/bryo/bryogen.html>.
30. Calcott, M. J., Ackerley, D. F., Knight, A., Keyzers, R. A. & Owen, J. G. Secondary metabolism in the lichen symbiosis. *Chem. Soc. Rev.* **47**, 1730–1760 (2018).
31. Air Pollution Information System. Impacts of air pollution on lichens and bryophytes.
<http://www.apis.ac.uk/impacts-air-pollution-lichens-and-bryophytes-mosses-and-liverworts>.
32. US Forest Service. What Are Ferns?
<https://www.fs.fed.us/wildflowers/beauty/ferns/what.shtml>.
33. Climate change in the Northwest: implications for our landscapes, waters, and communities. *Choice Rev. Online* **51**, 51-6191-51–6191 (2014).
34. North Carolina Climate Office. Composition of the Atmosphere.
<https://webcache.googleusercontent.com/search?q=cache:dB8bn3PH4GAJ:https://cli>

mate.ncsu.edu/edu/Composition+&cd=30&hl=en&ct=clnk&gl=us&client=firefox-b-1-d.

35. American Chemical Society. Properties. *American Chemical Society*
<https://www.acs.org/content/acs/en/climatescience/greenhousegases/properties.html>.
36. NASA. Graphic: The relentless rise of carbon dioxide. *Climate Change: Vital Signs of the Planet* https://climate.nasa.gov/climate_resources/24/graphic-the-relentless-rise-of-carbon-dioxide.
37. National Centers for Environmental Information. National Trends: Temperature, Precipitation, and Drought. <https://www.ncdc.noaa.gov/temp-and-precip/us-trends/tmax/jul>.
38. Brodersen, C. R., McElrone, A. J., Choat, B., Matthews, M. A. & Shackel, K. A. The Dynamics of Embolism Repair in Xylem: In Vivo Visualizations Using High-Resolution Computed Tomography. *Plant Physiol.* **154**, 1088–1095 (2010).
39. Tyree, M. T. & Zimmermann, M. H. The Cohesion-Tension Theory of Sap Ascent. in *Xylem Structure and the Ascent of Sap* 49–88 (Springer Berlin Heidelberg, 2002). doi:10.1007/978-3-662-04931-0_3.
40. Hacke, U. G., Sperry, J. S., Pockman, W. T., Davis, S. D. & McCulloh, K. A. Trends in wood density and structure are linked to prevention of xylem implosion by negative pressure. *Oecologia* **126**, 457–461 (2001).
41. Venturas, M. D., Sperry, J. S. & Hacke, U. G. Plant xylem hydraulics: What we understand, current research, and future challenges. *J. Integr. Plant Biol.* **59**, 356–389 (2017).
42. Sperry, J. S., Donnelly, J. R. & Tyree, M. T. A method for measuring hydraulic conductivity and embolism in xylem. *Plant Cell Environ.* **11**, 35–40 (1988).
43. Venturas, M. D. *et al.* Direct comparison of four methods to construct xylem vulnerability curves: Differences among techniques are linked to vessel network characteristics. *Plant Cell Environ.* **42**, 2422–2436 (2019).
44. Koch, G. W., Sillett, S. C., Jennings, G. M. & Davis, S. D. The limits to tree height. *Nature* **428**, 851–854 (2004).
45. Olson, M. E. *et al.* Plant height and hydraulic vulnerability to drought and cold. *Proc. Natl. Acad. Sci.* **115**, 7551–7556 (2018).
46. Ambrose, A. R., Sillett, S. C. & Dawson, T. E. Effects of tree height on branch hydraulics, leaf structure and gas exchange in California redwoods. *Plant Cell Environ.* **32**, 743–757 (2009).
47. Holbrook, N. M. & Zwieniecki, M. A. Embolism Repair and Xylem Tension: Do We Need a Miracle? *Plant Physiol.* **120**, 7–10 (1999).
48. Brase, C. & Price, G. Hydraulic Response to Heat in the Urban Forest as a Proxy for Future Acclimation to Climate Change. (2019).
49. Choat, B. *et al.* Global convergence in the vulnerability of forests to drought. *Nature* **491**, 752–755 (2012).